0026-895X/95/020362-17$3.00/0

MOLECULAR PHARMACOLOGY, 48:362–378 (1995).

Detection, Quantitation, and Verification of Allosteric Interactions of Agents with Labeled and Unlabeled Ligands at G Protein-Coupled Receptors: Interactions of Strychnine and Acetylcholine at Muscarinic Receptors

SEBASTIAN LAZARENO and NIGEL J. M. BIRDSALL

Medical Research Council Collaborative Centre, London, NW7 1AD, UK (S.L.), and Division of Physical Biochemistry, National Institute for Medical Research, London, NW7 1AA, UK (N.J.M.B.)

Received December 19, 1994; Accepted May 22, 1995

SUMMARY

Novel methods of detecting and quantitating cooperative interactions between an agent and both a tritiated (muscarinic) antagonist and the endogenous agonist (acetylcholine), acting at a common (muscarinic) receptor, have been devised. In a semiquantitative protocol, binding data are transformed into affinity ratios (the ratios of the apparent affinity of the ligand in the presence of the agent to the affinity of the ligand alone), which allow estimates to be made of the potency of the agent and its cooperativity with the tritiated antagonist and with the unlabeled ligand. These parameters have been quantitated by detailed binding assays or guanosine-5′-*O*-(3-[^{35}S]thio)triphosphate functional assays. The kinetic phenomena associated with the allosteric interactions have been exploited in two nonequilibrium binding assays, from which the affinity constants describing the allosteric interactions can be extracted. The different assay methods give quantitatively similar and internally consistent estimates of the parameters describing the cooperative interactions. Using these assays, strychnine has been found to act allosterically at muscarinic receptors. Strychnine has an affinity of $\sim 10^5$ M^{-1} at the unliganded m1, m2, and m4 receptors but is 5–10-fold weaker at m3 receptors. It is positively cooperative with *N*-methylscopolamine at m2 and m4 receptors and exhibits neutral and negative cooperativity with m1 and m3 receptors, respectively. With acetylcholine, it is negatively cooperative but the degree of cooperativity is relatively low (2–7-fold), particularly at m1 and m4 receptors. The methods and equations described should be useful in detecting and quantitating allosteric interactions of agents with the endogenous neurotransmitter at G protein-coupled receptors.

There are five subtypes of muscarinic ACh receptors, which exhibit a strong conservation of sequence in those regions that are considered to bind agonists and antagonists (1). As a consequence, it has proven difficult to discover agents that are highly selective for just one subtype.

Muscarinic receptors also possess a second, allosteric, binding site (2–4). The binding of ligands to this site changes the affinity of, but does not abolish, the binding of ligands to the competitive site (2, 5–7). Gallamine, the first allosteric ligand to be examined in detail, decreases the binding of many antagonists and agonists (2, 8). In contrast it has recently been reported that alcuronium, a neuromuscular blocker, enhances the binding of the antagonist NMS to M_2 but not M_3 receptors by an allosteric mechanism (9, 10). However, alcuronium decreases the binding of agonists.

Because the allosteric interaction involves the simultaneous binding of the allosteric ligand and competitive agent (agonist or antagonist) to the receptor, the allosteric site and the competitive site are necessarily different. It is therefore conceivable that there could be greater sequence differences between the allosteric sites on the receptor subtypes than are present at the conventional competitive sites, providing a prospect of developing agents with greater subtype selectivity.

Allosteric drugs can regulate receptor function in selective and very different ways, compared with agonists and antagonists. Particularly important are the allosteric interactions between the endogenous neurotransmitter and the allosteric ligand. This is because of the potential therapeutic importance and selectivity of such agents (11, 12).

For the development of such agents into potential drugs, it is necessary to obtain quantitative binding data to establish the relevant structure-activity relationships. In the case of allosteric agents this is particularly difficult, because two parameters, i.e., the affinity of the agent for the unliganded receptor and the cooperativity of its binding to neurotrans-

ABBREVIATIONS: ACh, acetylcholine; NMS, *N*-methylscopolamine; QNB, 3-quinuclidinylbenzilate; GTPγS, guanosine-5′-*O*-(3-thio)triphosphate; GABA, γ-aminobutyric acid; HEPES, 4-(2-hydroxyethyl)-1-piperazineethanesulfonic acid.

mitter-occupied receptor to generate the ternary complex, are required to define the interaction. The situation is even more complex when a third, radiolabeled, ligand must be used to detect the allosteric interaction between an allosteric agent and the neurotransmitter, because the effect of an allosteric agent depends, both quantitatively and qualitatively, on the particular ligand occupying the 'primary' binding site (2, 9).

In this paper we present several novel methods for detecting and quantitating the allosteric interactions between ACh and allosteric agents acting at muscarinic receptor subtypes. As one of our main examples, we use strychnine, an unanticipated allosteric muscarinic agent,[1] which in the simplest terms may be viewed as a monomer of a functionalized dimer, alcuronium.

The methods described in this paper can be applied to generate quantitative data on allosteric interactions at other G protein-coupled receptors. The equations that describe the allosteric interactions and underpin the analysis of the experimental data are presented in the Appendix.

Experimental Procedures

Materials

[^{3}H]NMS (84–86 Ci/mmol) was from Amersham International, and [^{3}H]ACh (75–85 Ci/mmol) was from Amersham International or ARC Inc. (St. Louis, MO). Strychnine HCl, ACh chloride, and gallamine triethiodide were from Sigma Chemical Co., and alcuronium chloride was a kind gift from Roche Products.

Cell Culture and Membrane Preparation

Chinese hamster ovary cells stably expressing cDNA encoding human muscarinic m1–m4 receptors (13) were generously provided by Dr. N. J. Buckley (National Institute for Medical Research, London, UK). These were grown in α-minimal essential medium (Gibco) containing 10% (v/v) newborn calf serum, 50 units/ml penicillin, 50 μg/ml streptomycin, and 2 mM glutamine, at 37° under 5% CO_2. Cells were grown to confluence and harvested by scraping in a hypotonic medium (20 mM HEPES, 10 mM EDTA, pH 7.4). Membranes were prepared at 0° by homogenization (with a Polytron homogenizer) followed by centrifugation (at 40,000 × g for 15 min), washed once in 20 mM HEPES, 0.1 mM EDTA, pH 7.4, and stored at −70° in the same buffer. Protein concentrations were measured with the Bio-Rad reagent, using bovine serum albumin as the standard. The yields of receptor varied from batch to batch but were approximately 5, 1, 7, and 2 pmol/mg of total membrane protein for the m1, m2, m3, and m4 subtypes, respectively.

Radioligand Binding Assays

Unless otherwise stated, frozen membranes were thawed, resuspended in a buffer containing 20 mM HEPES, 100 mM NaCl, and 10 mM $MgCl_2$, pH 7.4, and incubated with radioligand and unlabeled drugs for 2 hr at 30°, in a volume of 1 ml. Membranes were collected by filtration (using a Brandel cell harvester; Brandel, Semat, Herts, UK) over glass fiber filters (Whatman GF/B filters that had been presoaked in 0.1% polyethylenimine), extracted overnight in scintillation fluid (ReadySolve; Beckman), and counted for radioactivity in Beckman LS6000 scintillation counters. Membrane protein concentrations (5–50 μg/ml) were adjusted so that not more than approximately 15% of added radioligand was bound. Nonspecific binding was measured in the presence of 1 μM QNB (an antagonist with picomolar potency) and accounted for 1–5% of total binding. In some assays GTP was present at a concentration of 0.2 mM. Data points were usually measured in duplicate. Chinese hamster ovary cell membranes do not possess cholinesterase activity,[2] so ACh could be used in the absence of a cholinesterase inhibitor.

Equilibrium Radioligand Binding Assays

Semiquantitative estimation of the cooperativity between an agent and both [^{3}H]NMS and unlabeled ACh and the affinity of the agent for the receptor. Binding data were obtained with a high concentration of [^{3}H]NMS (2–3 nM) and with a low concentration of [^{3}H]NMS (0.2 nM for m1, m3, and m4 receptors and 0.4 nM for m2 receptors), in the absence and presence of a number of concentrations of the agent (typically three concentrations), in the absence and presence of a fixed concentration of ACh (20 μM for m1 and m3 receptors, 2 μM for m2 receptors, and 5 μM for m4 receptors). These data were transformed into 'affinity ratios,' i.e., ratios of the apparent affinity of the ligand ([^{3}H]NMS or ACh) in the presence of the agent to the affinity of the ligand alone. This affinity ratio measure is, in principle, independent of the fixed concentration of ligand. It also follows the receptor occupancy of the agent, so that if the agent is competitive or strongly negatively allosteric the IC_{50} corresponds to the dissociation constant of the agent at the free receptor in the absence of other ligands.

The calculations were as follows. Specific binding was obtained by subtracting nonspecific from total binding. Free radioligand (in dpm) was obtained by subtracting total binding with [^{3}H]NMS alone from the amount of added radioligand. The B_{max} was calculated using eq. 7 (see Appendix). Specific binding data in the absence and presence of ACh were transformed into apparent affinities of [^{3}H]NMS and ACh using eqs. 9 and 13, respectively (see Appendix). These apparent affinities were divided by the true affinity (in the absence of agent) to obtain the affinity ratios r_{NMS} and r_{ACh}. Values of r greater than 1 suggest the presence of positive cooperativity. Values of r less than 1 for which the asymptotic value, at high concentrations of agent, is greater than 0 suggest weak negative cooperativity, whereas values of r less than 1 that tend to an asymptote of 0 suggest strong negative cooperativity or a competitive interaction.

The assay was conducted in the presence of 0.2 mM GTP, to minimize high affinity ACh binding. Nevertheless, the Hill slopes of ACh inhibition curves under these conditions were less than 1 (~0.8–1) for all subtypes, which violates one of the assumptions of the analysis (that the Hill slope of ACh binding is 1). Although this violation may introduce a small quantitative error into the estimates of relative ACh affinity, in practice the error seems to be negligible, because overlapping curves for affinity ratios of [^{3}H]NMS and ACh were obtained when the agent was a competitive antagonist (Fig. 1b).

Measurement of the influence of an agent on [^{3}H]ACh binding. Binding of [^{3}H]ACh to m2 receptors (600 μg of protein/ml) and m4 receptors (600 μg of protein/ml) was measured after an incubation of 1 hr in a volume of 250 μl. The assay did not contain GTP and therefore measured the interaction of the agent with the ACh-receptor-G protein ternary complex. It was practical to carry out these experiments only with m2 and m4 receptors, because little specific [^{3}H]ACh binding to m1 or m3 receptors could be detected. The K_d and B_{max} of [^{3}H]ACh binding may be altered by perturbations of receptor-G protein coupling, so we did not attempt to express changes in [^{3}H]ACh binding as affinity ratios. Instead, bound [^{3}H]ACh in the presence of a number of concentrations of the agent (typically three concentrations) was expressed simply as a fraction of control [^{3}H]ACh binding. Concentrations of [^{3}H]ACh less than or equal to its dissociation constant (K_d of ~1 nM at m2 receptors and ~10 nM at m4 receptors) were used, so curves obtained with this assay are predicted to lie not more than 0.3 log units to the right of affinity ratio curves obtained with unlabeled ACh using the semiquantitative assay.

Equilibrium assay for quantitative estimation of the affinity of an allosteric agent for the receptor and the magnitude of its cooperativity with [^{3}H]NMS and ACh. The assay contained

[1] P. Gharagozloo, S. Lazareno, A. Popham, T. Farries, M. Sugimoto, and N. J. M. Birdsall. Allosteric interactions of strychnine analogues with muscarinic receptors. Manuscript in preparation.

[2] S. Lazareno, unpublished observations.

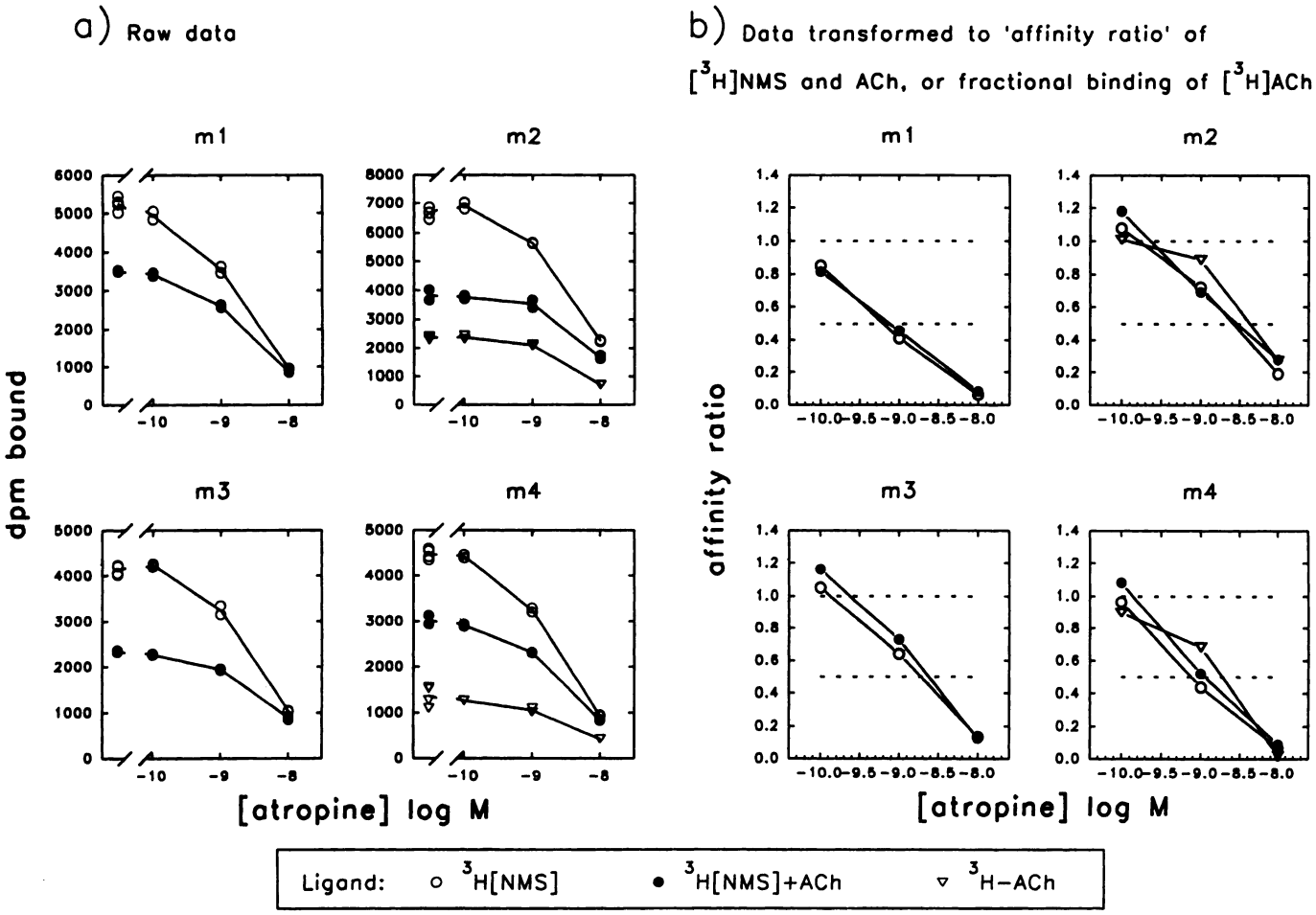

Fig. 1. a, Effect of atropine on the binding of [^{3}H]NMS in the absence (○) and presence (●) of ACh at m1–m4 receptors and on the binding of [^{3}H]ACh (▽) at m2 and m4 receptors. Nonspecific binding was 50–150 dpm. Total binding and nonspecific binding of a high concentration of [^{3}H]NMS were also measured, allowing the data to be converted to apparent affinities (see Experimental Procedures and Appendix, section C). [^{3}H]NMS binding was measured in the presence of 0.2 mM GTP. Individual data points from a single experiment, which was repeated once, are shown. b, Same data as in a, transformed to affinity ratios for [^{3}H]NMS (○) and ACh (●) or fractional binding for [^{3}H]ACh (▽). *Dashed lines*, indicating affinity ratio levels of 1 and 0.5, are included as a guide to the eye.

0.2 mM GTP to measure, as far as possible, effects that were independent of G protein coupling. The binding of [^{3}H]NMS (0.2 nM for m1, m3, and m4 receptors, 0.4 nM for m2 receptors, or as stated) was measured alone and in the presence of six concentrations of ACh, alone and in the presence of three concentrations of test agent. Binding with a high concentration of [^{3}H]NMS was also measured, allowing the B_{max} to be estimated using eq. 7 (see Appendix). The specific binding data and estimated B_{max} were subjected to nonlinear regression analysis using eq. 34 (see Appendix). Above a certain concentration, some allosteric agents, especially those that are neutrally or positively cooperative with [^{3}H]NMS, may slow the kinetics of [^{3}H]NMS binding so much that the binding does not reach equilibrium. Knowledge of the affinity of the agent for the [^{3}H]NMS-occupied receptor allows the maximum 'safe' concentration of agent to be estimated (see Appendix, eq. 31). The strychnine and [^{3}H]NMS concentrations and incubation time used (see the legend to Table 3) were chosen to minimize the predicted effects of strychnine on [^{3}H]NMS association kinetics. It is possible that [^{3}H]NMS binding in the presence of the highest strychnine concentration and strongly inhibitory concentrations of ACh does not reach equilibrium, but small errors in these values do not significantly perturb the analysis.

Estimation of the affinity of an allosteric agent for the [^{3}H]NMS-occupied receptor.

Unless otherwise stated, a high concentration of membranes (2–4 mg of protein/ml) was incubated with a high concentration of [^{3}H]NMS (5 nM) for about 15 min. Then 10-μl aliquots were distributed to tubes, which were empty or contained 100 μl of 10^{-6} M QNB alone or in the presence of a number of concentrations of allosteric agent (typically four concentrations). Nonspecific binding was measured in separately prepared tubes containing 10 μl of membranes and 2 μl of [^{3}H]NMS plus QNB. Some time (about 2.5 dissociation half-lives) later (see Table 4), the samples were filtered. The data were transformed to rate constants, k_{off}, using the formula

$$k_{off} = \ln(B_0/B_t)/t$$

where B_0 is initially bound radioligand and B_t is bound radioligand after t minutes of dissociation. These values were finally expressed as percentage inhibition of the true [^{3}H]NMS dissociation rate constant (k_{off} in the absence of allosteric agent) and fitted to a hyperbolic function using nonlinear regression analysis. This curve corresponds to the occupancy curve for the allosteric agent at the [^{3}H]NMS-occupied site (see Appendix, section E2). When the dissociation of [^{3}H]NMS was measured as a function of time, the binding reaction was started at different times to ensure that the same association time was used for all dissociation times.

Nonequilibrium Assay to Detect and Use the Slowing of [^{3}H]NMS Association Kinetics by an Allosteric Agent

Solutions/suspensions of [^{3}H]NMS and membranes were prepared at 100 times their final concentration. Prelabeling of receptors was achieved by mixing a portion of the [^{3}H]NMS solution and membrane suspension; the concentration of [^{3}H]NMS in the mixture was 50 times greater than its final concentration so that, unless the final concentration was very low, almost the entire receptor population was labeled within 1 or 2 min. Tubes were prepared containing 1 ml of allosteric agent at its final concentration, in the absence or presence of a fixed concentration of ACh. GTP (0.2 mM) was present throughout.

The incubation was initiated by adding membranes or the membrane/[^{3}H]NMS mixture to the appropriate set of tubes. There were three sets of tubes. Set A tubes did not contain ACh and received 20 μl of the membrane/[^{3}H]NMS mixture, which had been prepared at least 5 min before. Set B tubes also did not contain ACh and received 10 μl of [^{3}H]NMS, followed by 10 μl of membranes. Set C tubes were like set B but in addition contained ACh. The incubation proceeded at 30° for about 10 [^{3}H]NMS dissociation half-lives (see Table 5 and the legend to Fig. 7). After dilution with allosteric agent, set A tubes attained equilibrium by dissociation of [^{3}H]NMS. Kinetic slowing effects in set A tubes were seen as an increase in binding above the equilibrium level, whereas the equivalent effects in set B and set C tubes were seen as decreased binding. The data for all sets of tubes were analyzed simultaneously by nonlinear regression using eqs. 33, 27, or 30 as appropriate (see Appendix, section G).

[^{35}S]GTPγS Binding Assays

Membranes (5–20 μg/ml) were incubated with [^{35}S]GTPγS (0.1 nM), GDP 0.1 μM for m1 and m3 receptors and 1 μM for m2 and m4 receptors), and ligands, in a volume of 1 ml, for 30 min at 30°. Bound label was collected by filtration over prewetted (with water) glass fiber filters. Concentration-response curves for ACh were fitted to logistic functions or to the allosteric model (Appendix, section H, eq. 37).

Data Analysis

The affinity ratio calculations and plots were made using Minitab (CLECOM Ltd., Birmingham, UK). Nonlinear regression analyses were performed using the fitting procedure in SigmaPlot (Jandel Scientific, Erkrath, Germany). This procedure is relatively powerful, in that it allows the use of two or more independent variables, e.g., concentrations of two drugs; this facility is required for most of the analyses described here.

Results

Equilibrium Binding Assays

Semiquantitative assay. This assay allows the effect of an agent on [^{3}H]NMS binding to be directly compared with its effect on unlabeled ACh binding. This is achieved by calculating the apparent affinity of [^{3}H]NMS and ACh in the presence of a particular concentration of agent and expressing it as a fraction of the affinity of the ligand in the absence of agent, as described in Experimental Procedures and Appendix, section C. This affinity ratio measure, in principle, follows the receptor occupancy of the agent in the absence of other ligands (Appendix, section D). Therefore, if the agent is a competitive antagonist or has strong negative cooperativity with [^{3}H]NMS and ACh, the affinity ratio curves for [^{3}H]NMS and ACh should overlap and have an IC_{50} value corresponding to the K_d of the agent. If, however, the affinity ratio curves diverge, this suggests that the agent may be acting allosterically.

The effect of the agent on direct [^{3}H]ACh binding at m2 and m4 receptors can also be measured, which provides a check on the validity of the assay. An internal check is also provided by the single-point estimates of the [^{3}H]NMS dissociation constant (K_d) and B_{max} and the ACh pK_i obtained from each assay (Table 1). For illustrative purposes we describe the properties of a competitive antagonist and an allosteric agent in this assay.

Fig. 1 shows the effect of atropine, a competitive antagonist, on [^{3}H]NMS binding, alone and in the presence of ACh, at m1–m4 receptors and its effect on [^{3}H]ACh binding at m2 and m4 receptors. Fig. 1a shows the raw data, and Fig. 1b shows the [^{3}H]NMS data transformed into affinity ratios (see Experimental Procedures and Appendix, section C). As predicted for a competitive antagonist such as atropine, the inhibition curves for unlabeled ACh and [^{3}H]NMS affinity ratios overlap, whereas the curves with [^{3}H]ACh at m2 and m4 receptors (which show fractional binding rather than affinity ratios) (see Experimental Procedures) lie slightly to the right.

As mentioned above, the IC_{50} values of the affinity ratio curves correspond theoretically to the K_d (1/affinity) of the competitive antagonist. Table 2 shows affinity estimates for atropine from two experiments, obtained by visual inspection of the graphs. The estimates obtained using the ACh and [^{3}H]NMS data are almost identical. Table 2 also shows the values obtained by fitting the raw data to a hyperbolic function and applying the appropriate Cheng-Prusoff correction.

TABLE 1

Single-point estimates of [^{3}H]NMS K_d and ACh log affinity values (pK_i) from the semiquantitative assay (protocol 1)

Values are the mean ± standard error of five experiments.

	m1	m2	m3	m4
[^{3}H]NMS K_d (pM)	120 ± 9	324 ± 16	218 ± 10	79 ± 2
ACh pK_i (−log M)	4.90 ± 0.11	5.95 ± 0.04	5.00 ± 0.09	5.59 ± 0.05

TABLE 2

Estimates of atropine log affinity values from the semiquantitative assay shown in Fig. 1 and a similar repeat experiment

Affinity estimates (mean ± range/2) were obtained from the three-point inhibition curves for atropine versus [^{3}H]NMS, both in the absence and in the presence of ACh (see Experimental Procedures). The values were obtained both by visual inspection of the affinity ratio plots and by analysis of the raw data.

	Log affinity			
	Affinity ratio plot[a]		Hyperbolic function[b]	
	[^{3}H]NMS alone	[^{3}H]NMS + ACh	[^{3}H]NMS alone	[^{3}H]NMS + ACh
m1	9.17 ± 0.03	9.10 ± 0	9.17 ± 0.02	9.21 ± 0.01
m2	8.57 ± 0.03	8.53 ± 0.03	8.62 ± 0.02	8.67 ± 0.02
m3	8.75 ± 0.05	8.65 ± 0.05	8.85 ± 0.06	8.88 ± 0.07
m4	9.17 ± 0.07	9.20 ± 0.20	9.14 ± 0.01	9.16 ± 0.02

[a] The concentration of atropine causing an affinity ratio of 0.5 was determined from the affinity ratio plots (see Fig. 1) by visual inspection.

[b] The raw data were fitted to a hyperbolic function to obtain the IC_{50} of atropine, which was converted to an estimate of K_i with the appropriate form of the Cheng-Prusoff correction, i.e., $K_i = IC_{50}/(1 + [[^3H]NMS]/K_{d_{NMS}})$ for atropine versus [^{3}H]NMS or $K_i = IC_{50}/(1 + [[^3H]NMS]/K_{d_{NMS}} + [ACh]/K_{d_{ACh}})$ for atropine versus [^{3}H]NMS plus ACh. The values of $K_{d_{NMS}}$ and $K_{d_{ACh}}$ used to transform IC_{50} values were single-point estimates obtained within the same experiment (see Experimental Procedures), and a summary of these values, together with corresponding values from three other assays (using strychnine), is shown in Table 1.

Again, these values are almost identical to those obtained from the affinity ratio plot, confirming that, for an antagonist, this measure does correspond to (1 − fractional receptor occupancy) for the agent in the absence of competing ligands.

Fig. 2 shows similar data obtained with strychnine, an allosteric agent. At 10^{-4} M, strychnine slightly inhibited [^{3}H]NMS affinity at m1 and m3 receptors. At 10^{-5} and 10^{-4} M, it clearly enhanced [^{3}H]NMS binding at m2 and m4 receptors. It had a negative effect on ACh affinity at all subtypes, as measured with both unlabeled and labeled ACh.

The small effects of strychnine on the [^{3}H]NMS affinity ratio at m1 and m3 receptors, seen only at 10^{-4} M, suggest that strychnine either is neutrally cooperative with [^{3}H]NMS or is a weak allosteric inhibitor. These possibilities can be distinguished by considering the results of this assay in conjunction with those obtained in the [^{3}H]NMS dissociation assays (which measure the effect of the agent on the [^{3}H]NMS-occupied receptor; see below). The logarithm of its affinity for the [^{3}H]NMS-occupied m1 receptor is about 5 (see Table 4), so if strychnine were negatively cooperative it would have a log affinity of >5 for the free receptor and inhibition would be seen at a strychnine concentration of 10^{-5} M. In fact, no inhibition was seen at this concentration, and therefore strychnine is probably neutrally cooperative with [^{3}H]NMS at m1 receptors; the small inhibition at 10^{-4} M is possibly a kinetic artifact (see below). The analysis of the data at this concentration in the presence of ACh may therefore be unreliable, although strychnine is clearly inhibitory with ACh at m1 receptors.

Strychnine at 10^{-4} M also slightly inhibited [^{3}H]NMS binding at m3 receptors. The logarithm of the affinity of strychnine at [^{3}H]NMS-occupied m3 receptors was about 4.2 (see Table 4), so 10^{-4} M strychnine would not cause a slowing of the [^{3}H]NMS association rate sufficient to cause a kinetic artifact. The inhibition of [^{3}H]NMS binding at m3 receptors is probably the manifestation of a small negative allosteric effect, whereas there appears to be relatively large negative cooperativity with ACh.

Quantitative assay. This assay measures ACh inhibition of [^{3}H]NMS binding in the absence and presence of three or four concentrations of the agent, all in the presence of 0.2 mM GTP. The raw data are subjected to nonlinear regression analysis, as described in Experimental Procedures, to yield estimates of the affinity of the agent at the free receptor and its cooperativity with [^{3}H]NMS and ACh. Using strychnine as the test agent, Fig. 3 shows the results of a representative experiment and Table 3 shows summary data from three experiments (except for m3, for which one experiment was

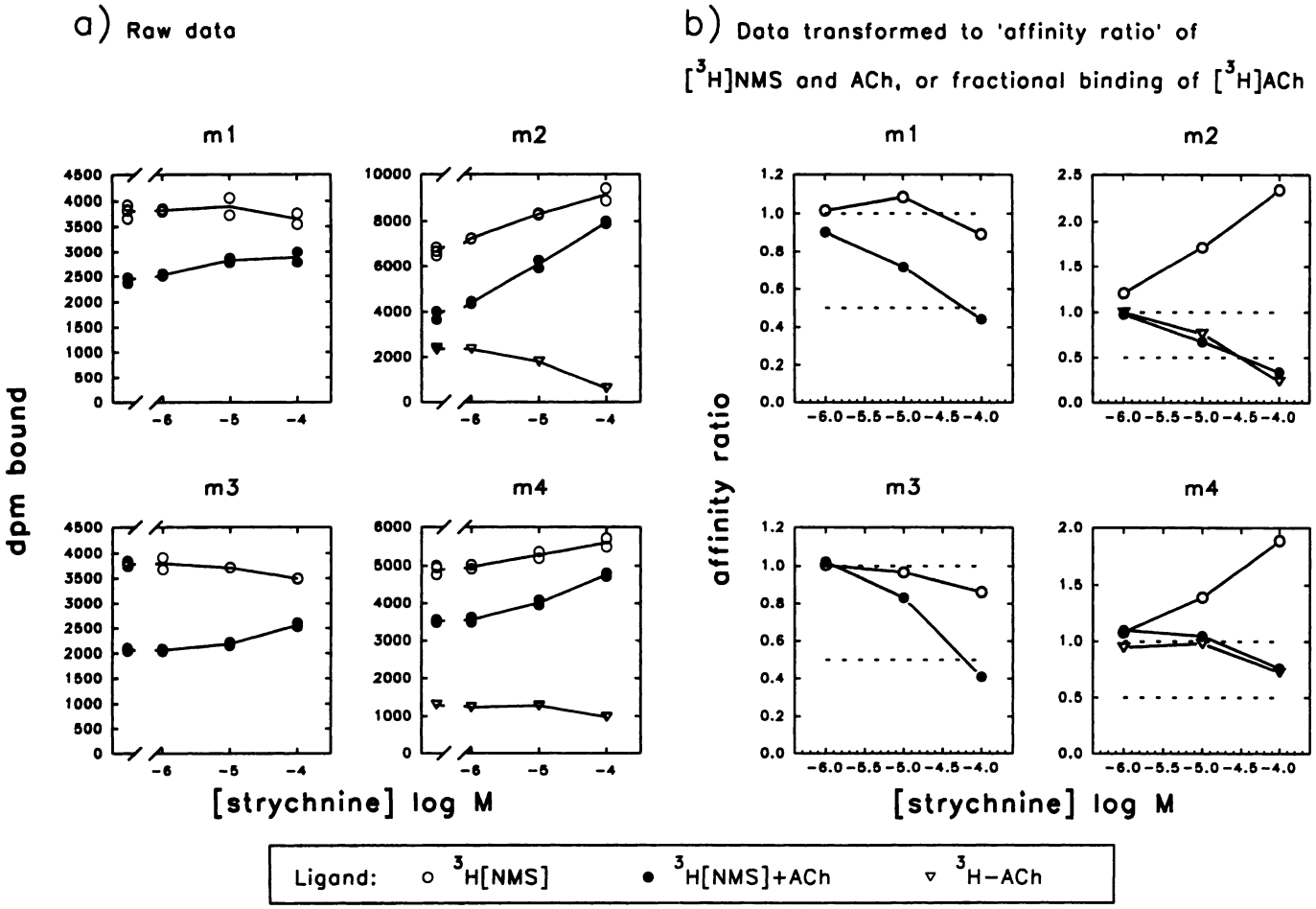

Fig. 2. a, Effect of strychnine on the binding of [^{3}H]NMS in the absence (○) and presence (●) of ACh at m1–m4 receptors and on the binding of [^{3}H]ACh (▽) at m2 and m4 receptors. See the legend to Fig. 1 for more details. The experiment was repeated twice with very similar results. b, Same data as in a, transformed to affinity ratios for [^{3}H]NMS (○) and ACh (●) or fractional binding for [^{3}H]ACh (▽).

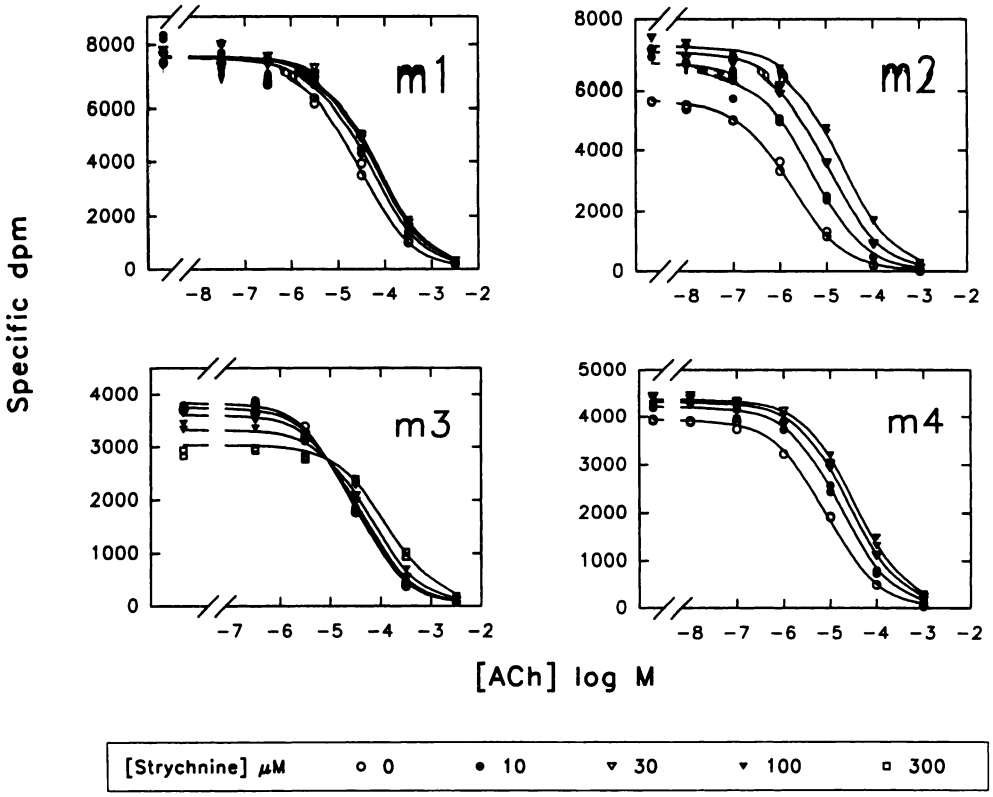

Fig. 3. Inhibition by ACh of [^{3}H]NMS binding in the absence and presence of three or four concentrations of strychnine, all in the presence of 0.2 mM GTP. Individual data points are shown. The *lines* indicate the fit of the allosteric model (eq. 34) to the data. See Table 3 for additional information.

TABLE 3

Parameters for the interaction of strychnine with [^{3}H]NMS and ACh at m1–m4 receptors

Values are the mean ± standard error of *n* experiments. Data were obtained using the quantitative equilibrium assay (see Experimental Procedures and Fig. 3). The K_d of [^{3}H]NMS was estimated in each assay, except for the assay with m3 receptors, which used the mean [^{3}H]NMS K_d shown in Table 1. The incubation times were 3.5–4 hr, and [^{3}H]NMS concentrations were as follows: m1, 360 ± 40 pM; m2, 440 ± 20 pM; m3, 204 pM; m4, 230 ± 10 pM. The expressions in parentheses refer to symbols used in the Appendix, eq. 34.

	m1	m2	m3	m4
n	4	4	1	4
[^{3}H]NMS K_d (pM) ($1/K_L$)	112 ± 13	305 ± 13		83 ± 9
ACh pK_i (−log M) (log K_A)	5.03 ± 0.08	6.17 ± 0.03	4.9	5.72 ± 0.09
ACh slope (n)	0.85 ± 0.02	0.78 ± 0.01	0.86	0.80 ± 0.01
Log affinity of strychnine for the free receptor (log K_X)	4.90 ± 0.21	4.96 ± 0.10	4.16	5.01 ± 0.06
Cooperativity with [^{3}H]NMS (α)	1.0 ± 0.1	2.2 ± 0.3	0.7	1.7 ± 0.1
Cooperativity with ACh (β)	0.41 ± 0.03	0.15 ± 0.02	<0.1	0.46 ± 0.05

performed). The results are completely compatible with the semiquantitative results and predictions described above and with the 'off-rate' assay (see below and Table 4). The cooperativity of strychnine with [^{3}H]NMS is neutral at m1, negative at m3, and positive at m2 and m4 receptors, whereas its cooperativity with ACh is negative at all subtypes (about 2-fold at m1 and m4 receptors and 6-fold or more at m2 and m3 receptors).

To confirm that the increased [^{3}H]NMS binding at m2 receptors in the presence of strychnine was caused by an increase in affinity, rather than B_{max}, binding of a range of concentrations of [^{3}H]NMS to m2 receptors was measured in

TABLE 4

Estimates of [^{3}H]NMS dissociation rate constant (k_{off}) and log affinity of strychnine for [^{3}H]NMS-occupied m1–m4 receptors (K_{occ})

[^{3}H]NMS dissociation was measured at a single time point, as described in Experimental Procedures (m1, 20 min; m2, 4 min; m3, 25 min; m4, 25 min). The assays shown in Fig. 4 (see legend for parameters) are also included as single experiments. K_{occ}, referred to in the Appendix as $\alpha \cdot K_X$, was also estimated from the equilibrium and nonequilibrium experiments. Values are the mean ± standard error of *n* experiments.

	m1	m2	m3	m4
n	3	3	3	4
[^{3}H]NMS k_{off} (min^{-1})	0.076 ± 0.003	0.40 ± 0.05	0.068 ± 0.004	0.08 ± 0.01
Strychnine K_{occ} (log M^{-1})	4.90 ± 0.02	5.21 ± 0.09	4.23 ± 0.01	5.04 ± 0.07
Strychnine K_{occ}[a,b] (log M^{-1})	4.90 ± 0.20	5.28 ± 0.05	4.02	5.23 ± 0.03
Strychnine K_{occ}[b,c] (log M^{-1})	5.00 ± 0.17	5.24 ± 0.05		5.07 ± 0.06

[a] From equilibrium assays (Table 3).
[b] Obtained by multiplying the affinity values of strychnine for the free receptor by the cooperativity factors with [^{3}H]NMS. *n* values are as shown in Tables 3 and 5.
[c] From nonequilibrium assays (Table 5).

the presence of various concentrations of strychnine. The data were well described by the allosteric model and yielded the following parameters (mean ± standard error, three experiments): [^{3}H]NMS K_d, 308 ± 20 pM; strychnine log affinity, 5.09 ± 0.15; strychnine cooperativity with [^{3}H]NMS, 2.4 ± 0.2. These values are in agreement with the corresponding parameter estimates for m2 receptors obtained in the quantitative equilibrium assay and shown in Table 3.

[^{3}H]NMS Dissociation Assays

The ability of allosteric agents such as gallamine to inhibit the dissociation of [^{3}H]NMS has provided a convenient and popular method for measuring the potency of allosteric agents, but it has not always been clear what measure to use, or what it means. According to the ternary complex model, [^{3}H]NMS can dissociate both from unoccupied receptors and from receptors simultaneously occupied by the allosteric agent. We have considered the effect of an allosteric agent on [^{3}H]NMS dissociation by using numerical simulation (data not shown). If the dissociation kinetics of the agent are fast, relative to those of [^{3}H]NMS, then [^{3}H]NMS dissociation in the presence of the agent is described by a single-exponential function, but if the agent has slow kinetics at the [^{3}H]NMS-occupied receptor then biphasic or complex dissociation curves are predicted. Fig. 4 shows dissociation curves for [^{3}H]NMS dissociation from m1–m4 receptors in the presence of various concentrations of strychnine. The data at each receptor were fitted to eq. 23 (see Appendix, section E1). In this model strychnine binds to the [^{3}H]NMS-occupied receptor with a Hill slope of 1, and [^{3}H]NMS dissociation follows an exponential function with a rate constant that is a function of strychnine occupancy. In all cases the model provides a good fit to the data and dissociation curves follow a monoexponential function, as do more detailed curves obtained in the presence of gallamine and alcuronium (data not shown).

It is convenient to estimate [^{3}H]NMS dissociation by measuring the [^{3}H]NMS bound at a single time point in the presence of a range of drug concentrations. In many studies, such data are subtracted from equilibrium binding values (B_0) and presented as percentage inhibition of control dissociation. Alternatively, each point can be expressed as a rate constant [$\ln(B_0/B_t)/t$] and expressed as percentage inhibition of the control rate constant (Fig. 5). Because [^{3}H]NMS dissociation was found to follow an exponential time course both in the absence and in the presence of strychnine, single-point estimates of the [^{3}H]NMS dissociation rate constant (k_{off}) should allow a measure that is independent of the particular time over which dissociation occurred. Fig. 5 shows the m4

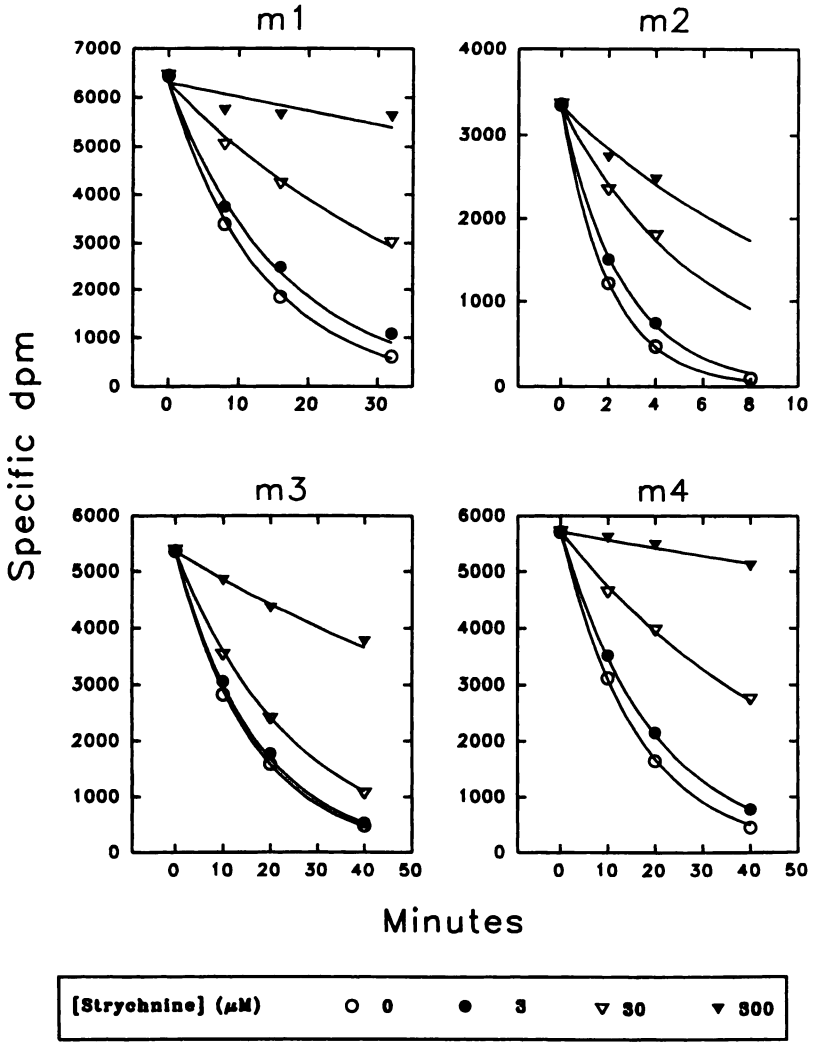

Fig. 4. Dissociation of [^{3}H]NMS in the presence of various concentrations of strychnine, measured at approximately 1, 2, and 4 dissociation half-lives. Each data point is the mean of duplicate measurements. The data were fitted to eq. 23 (see Appendix, section E1). The [^{3}H]NMS dissociation rate constant for the strychnine-occupied site was not statistically different from 0 except at m2 receptors, where k_{off_2} was 0.070 ± 0.006 min^{-1}. The fits are indicated by the *lines*, and estimates for [^{3}H]NMS k_{off} and the logarithm of the affinity of strychnine for the [^{3}H]NMS-occupied site were as follows: m1, 0.075 min^{-1} and 4.9; m2, 0.50 min^{-1} and 5.1; m3, 0.061 min^{-1} and 4.3; m4, 0.061 min^{-1} and 4.9, respectively.

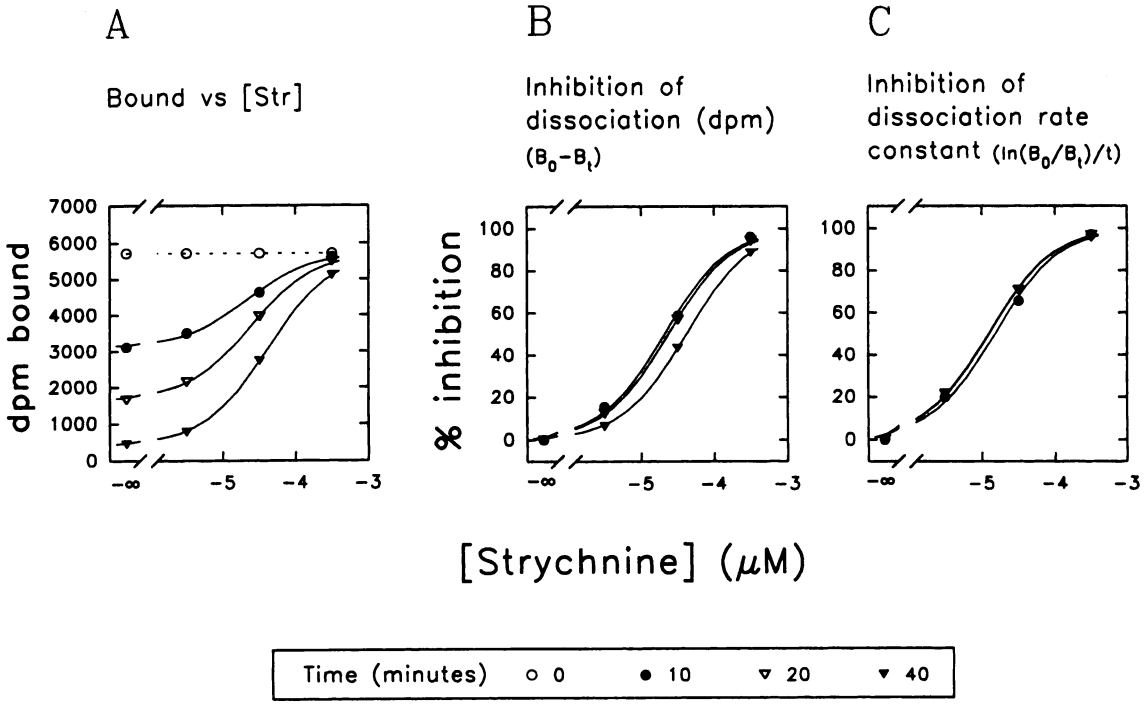

Fig. 5. Data for m4 shown in Fig. 4 but expressed as a function of strychnine (*Str*) concentration at each dissociation time. The data are shown untransformed (A), as percentage inhibition of control radioligand (dpm) dissociated (B), and as percentage inhibition of [^{3}H]NMS k_{off} (C). The *lines* show the fits to logistic functions.

data of Fig. 4 expressed as a function of strychnine concentration at different times. The individual curves were fitted to logistic functions, both as the raw data and as the data expressed as k_{off}; in both cases the logistic fits had slopes of about 1 (data not shown). The pIC_{50} values obtained from both types of curves for all subtypes are shown in Fig. 6 as a function of time. It can be seen that converting the data to rate constants provides a measure that is independent of time, whereas the pIC_{50} values obtained from the raw data are lower and decrease with time. These results confirm and extend recent observations with gallamine at m2 receptors (14).

As well as providing a time-independent measure of allosteric effects, the change in [^{3}H]NMS k_{off} in the presence of various concentrations of allosteric agent follows the occupancy by the agent of the [^{3}H]NMS-liganded receptor (see Appendix, section E2), so the pIC_{50} of this measure (or the pEC_{50} if the agent increases [^{3}H]NMS k_{off}) corresponds to the logarithm of the affinity of the agent for the [^{3}H]NMS-liganded receptor. Table 4 shows the summary results from the data of Fig. 4 and other experiments using a single time point, as described in Experimental Procedures. Table 4 also shows the estimates of the affinity of strychnine for the [^{3}H]NMS-occupied receptor obtained from the equilibrium experiments (Table 3) and nonequilibrium experiments (see below and Table 5). There is good agreement between the different types of assays.

Nonequilibrium Binding Assays

The ability of many allosteric agents to almost completely slow the dissociation kinetics of [^{3}H]NMS means that over the same concentration range they also slow its association kinetics. This is seldom a problem with negative allosteric agents because their inhibitory effects on equilibrium binding occur at lower concentrations than do their kinetic effects. With neutral or positive agents, however, concentrations that are effective in equilibrium assays may well slow [^{3}H]NMS kinetics such that binding equilibrium is not attained. Alcuronium stimulates, and then inhibits, [^{3}H]NMS binding to m2 receptors and the inhibition was initially attributed to competition (9), although those authors then demonstrated, by studying binding after different incubation times, that this is a kinetic artifact (10).

It is possible to detect and use kinetic artifacts with an assay in which radioligand binding equilibrium is attained from both directions, i.e., from unlabeled receptors and from prelabeled receptors (see Experimental Procedures and Appendix, section G). The kinetic effect of the agent is seen as an increase in binding with prelabeled receptors and a decrease in binding with initially unlabeled receptors. Both sets of data are fitted simultaneously to the appropriate equations (see Appendix, section G) to yield a number of parameters, including the affinity of the agent and its cooperativity with [^{3}H]NMS.

Fig. 7 shows the results of such an experiment with alcuronium at m2 receptors. The inhibition of binding seen at high concentrations is clearly a kinetic artifact. The estimates of the logarithm of alcuronium affinity and the cooperativity with [^{3}H]NMS (6.0 and 3.6, respectively) are consistent with the values (6.2 and 4.2) reported by Proška and Tuček (10) and the estimated log affinity for the [^{3}H]NMS-occupied receptor, 6.5, agrees well with values of 6.45 ± 0.05 (two experiments) obtained directly in [^{3}H]NMS dissociation assays.

The kinetic effects of even neutrally cooperative agents may cause problems with the quantitation of negative cooperativity with an unlabeled ligand, because high concentrations of agent are required to define large values of negative

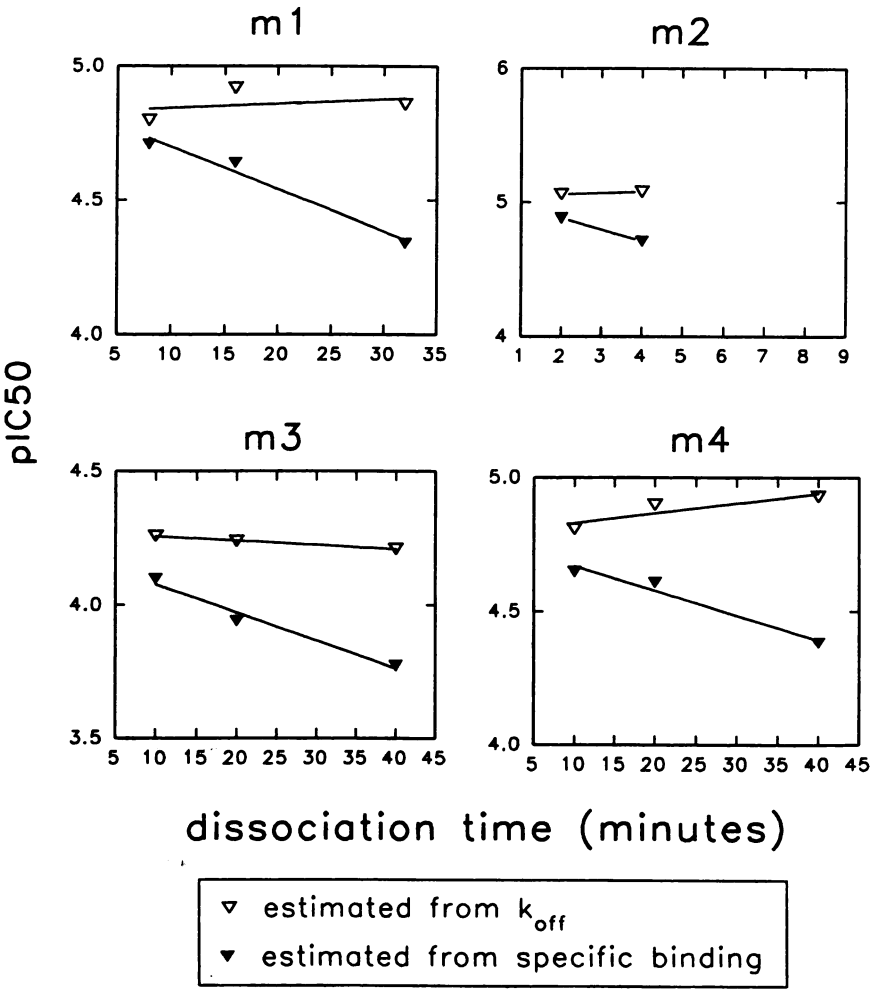

Fig. 6. pIC_{50} values from the logistic fits shown in Fig. 5, and similar fits with the data of the other receptor subtypes, as a function of dissociation time. Inhibition was calculated using both the calculated k_{off} values and the observed specific binding (dpm) values. The *lines* show linear regressions.

TABLE 5

Parameter estimates for strychnine at m1, m2, and m4 receptors from a nonequilibrium assay

One third of the samples contained receptors that had been prelabeled with [^{3}H]NMS before exposure to the allosteric agent, and half of the nonprelabeled samples contained ACh (100 μM for m1 receptors, 10 μM for m2 receptors, and 20 μM for m4 receptors). Incubation times were as follows: m1, 82 ± 4 min; m2, 29 ± 4 min; m4, 110 ± 11 min. [^{3}H]NMS concentrations were as follows: m1, 0.12 nM; m2, 0.32 nM; m4, 0.12 nM. The data were fitted to eqs. 33, 27, or 30 as appropriate (the off-rate of [^{3}H]NMS from the strychnine-occupied receptor was not different from 0 and was fixed at 0). Each assay was conducted in triplicate. Values are the mean ± standard error of *n* experiments.

	m1	m2	m4
n	3	3	4
Log affinity	5.13 ± 0.20	4.86 ± 0.05	4.78 ± 0.06
Cooperativity with [^{3}H]NMS	0.75 ± 0.05	2.43 ± 0.09	1.75 ± 0.19
Cooperativity with ACh	0.32 ± 0.04	0.05 ± 0.01	0.14 ± 0.02

cooperativity. In addition, the unlabeled inhibitor itself slows radioligand association (15). The nonequilibrium assay described above can be extended by adding a third set of tubes measuring binding to initially unlabeled receptors in the presence of a fixed concentration of unlabeled ligand. Including these data in the analysis allows an estimate of the cooperativity between the allosteric agent and unlabeled ligand. We have used this procedure to estimate the interactions of strychnine with ACh at m1, m2, and m4 receptors (in the presence of GTP).

Fig. 8 shows a representative experiment with each receptor subtype, and Table 5 summarizes the data obtained from a number of independent experiments. The parameter estimates from these experiments are in general agreement with those shown in Tables 3 and 4, except that the estimates of strychnine cooperativity with ACh were somewhat lower than those shown in Table 3. The model does not fit the data well at the highest concentrations of strychnine (Fig. 8); these deviations were consistently seen with strychnine, although not with alcuronium, and are probably a nonspecific effect of high strychnine concentrations.

Equilibrium assays would be impossible with agents that slow [^{3}H]NMS kinetics and have a greater degree of positive cooperativity with [^{3}H]NMS than is seen with strychnine, especially at m1, m3, or m4 receptors. The nonequilibrium assay described here allows the properties of such agents to be measured.

An agent could slow [^{3}H]NMS kinetics through two distinct mechanisms, i.e., an allosteric change in the shape of the receptor or steric hindrance to the access of [^{3}H]NMS to and egress from its binding site, as has been suggested (10, 16). It is worth noting that the kinetic methods we have described are equally valid for the two mechanisms, alone or in combination.

Functional [^{35}S]GTPγS Binding Assays

The functional consequence of ACh binding to its receptor, stimulation of guanine nucleotide exchange at one or more

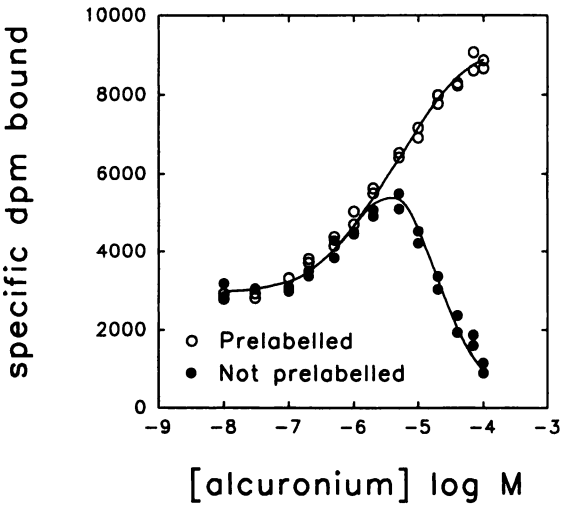

Fig. 7. Effect of alcuronium on [^{3}H]NMS (0.25 nM) binding to m2 receptors after a 40-min incubation. Receptors either were or were not prelabeled with [^{3}H]NMS before the incubation. Individual data points are shown, and the *lines* represent the simultaneous fit to eqs. 33 and 27 (see Experimental Procedures and Appendix, section G). The following parameters for alcuronium at m2 receptors were obtained from three independent experiments (mean ± standard error): log affinity for the free receptor, 6.00 ± 0.17; cooperativity with [^{3}H]NMS, 3.6 ± 0.7; log affinity for the [^{3}H]NMS-occupied receptor, 6.54 ± 0.10. In two of the three assays the data were significantly better fitted, as assessed with the extra sum of squares *F* test (31), when the rate of [^{3}H]NMS dissociation from the alcuronium-occupied receptor was included as a fitted parameter, yielding a value of 0.0011 ± 0.0004 min^{-1} (two experiments). This parameter was not different from 0 in the assays with strychnine. The values of affinity for the [^{3}H]NMS-occupied receptor were obtained by multiplying affinity for the free site and cooperativity.

classes of G protein, can be assessed by measuring the binding of a low concentration of [^{35}S]GTPγS in the presence of GDP (17, 18). This provides a convenient response for functionally assessing allosteric effects, using the same conditions as in the ligand binding studies.

The allosteric action of gallamine was first detected using a functional whole-tissue preparation (19), and Ehlert (8) used a second messenger response in membrane preparations to study in detail interactions between gallamine and two agonists. These and other studies have analyzed the dose ratio shifts in the presence of gallamine, or another agent, according to the current allosteric model. We have derived an equation that allows functional raw data to be fitted directly to the allosteric model, without the need to calculate dose ratio shifts (see Appendix, section H).

Gallamine reduced the potency of ACh for stimulating [^{35}S]GTPγS binding to m2 membranes but did not affect either basal activity or E_{max}, and the data were well fitted to the allosteric model (Fig. 9). From three independent experiments, the following parameter estimates were obtained (mean ± standard error): log affinity, 6.30 ± 0.05; cooperativity with ACh, 0.003 ± 0.001; −log EC_{50} for ACh, 7.6 ± 0.1; ACh slope, 0.9 ± 0.1. These results are similar to previously reported estimates of gallamine affinity at m2 receptors under comparable assay conditions in functional and binding studies (log affinities of 6.2 and 5.9, respectively) (2, 8) and cooperativity with ACh of 0.01 in a binding study (2).

Fig. 10 shows the effects of strychnine on ACh stimulation of [^{35}S]GTPγS binding to m1 and m2 membranes. Strychnine reduced ACh potency in a concentration-dependent manner, but to a greater extent and in a concentration range higher than that predicted from the [^{3}H]NMS binding experiments. At concentrations of 10^{-4} M and above, strychnine reduced E_{max} and basal levels, suggesting that it was inhibiting G protein function as well as binding to the allosteric site. These deviations from a simple allosteric effect do not allow a clear interpretation of the data.

Discussion

Agents affecting ion channel-coupled receptor activity through an allosteric action are well known; benzodiazepines, for example, enhance the affinity of GABA for the $GABA_A$ receptor. There are currently no drugs that are known to produce their therapeutic effects by allosteric ac-

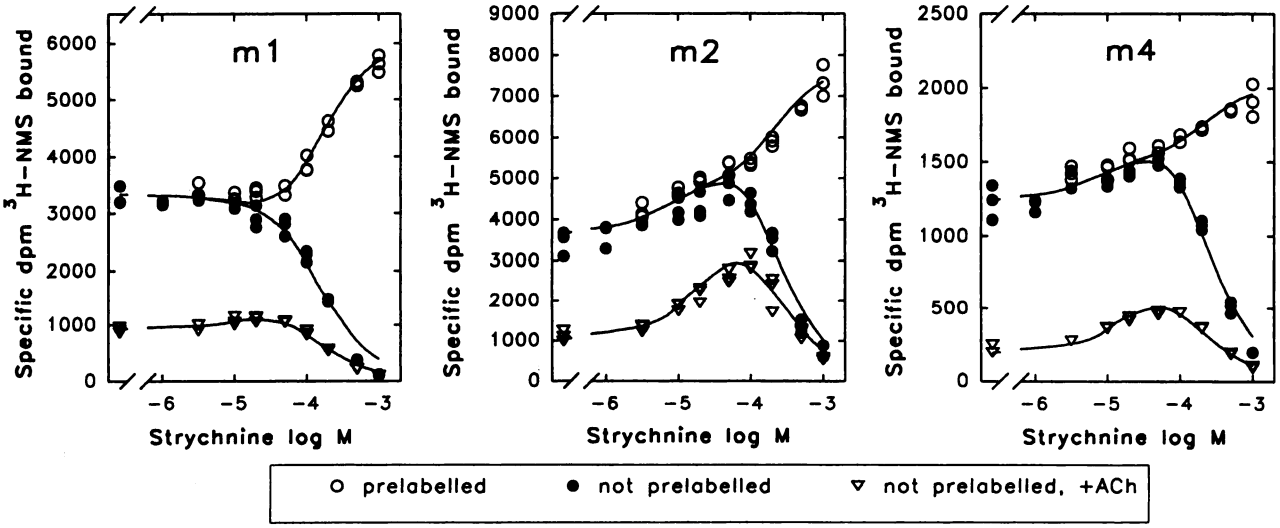

Fig. 8. Effect of strychnine on [^{3}H]NMS binding to m1, m2, and m4 receptors in the absence and presence of ACh. Receptors were either prelabeled with [^{3}H]NMS before the incubation, not prelabeled, or not prelabeled in the presence of ACh. The experiments were conducted in the presence of 0.1 mM GTP, in triplicate, and individual data points are shown. The *lines* show the simultaneous fit to eqs. 33, 27, and 30 (see Appendix, section G). See Table 5 for additional information.

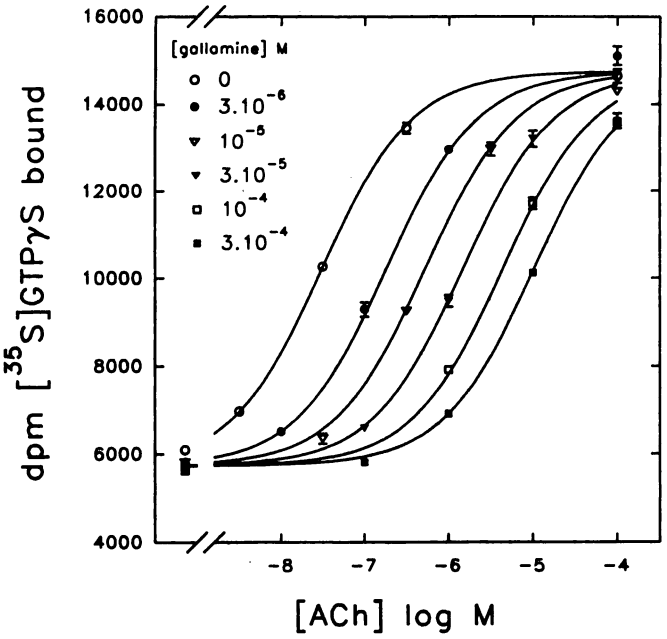

Fig. 9. Stimulation by ACh of [^{35}S]GTPγS (0.1 nM) binding to membranes containing m2 receptors, in the presence of 1 μM GDP and various concentrations of gallamine. The *points* show the means and standard errors of triplicate observations. The *lines* show the fits to the allosteric model (see Appendix, eq. 37).

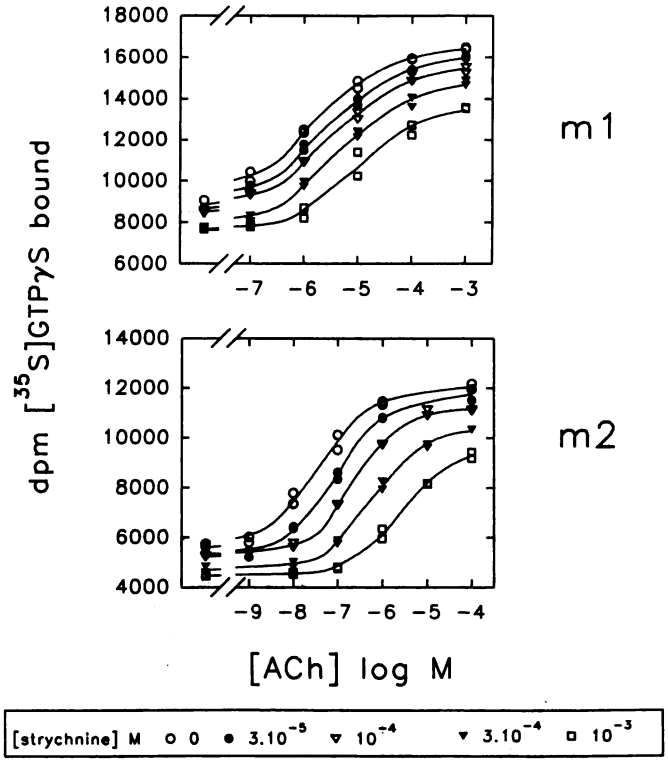

Fig. 10. Stimulation by ACh of [^{35}S]GTPγS (0.1 nM) binding to membranes containing m1 and m2 receptors, in the presence of 0.1 μM and 1 μM GDP, respectively, and various concentrations of strychnine. Individual data points are shown. The *lines* represent the logistic fit to each curve. The experiment was repeated with similar results.

tion at a G protein-coupled receptor, although such receptors are major targets of therapeutic drug action. There are, however, agents that may act allosterically at muscarinic, adenosine A_1, α_2-adrenergic, and dopamine D_2 receptors (4, 20–22).

It is impossible to predict the effects of an allosteric agent even with knowledge, or suspicion, of the role of the target receptor; benzodiazepines are highly effective and safe therapeutic agents (albeit with dependence liability), whereas directly acting $GABA_A$ agonists such as muscimol have not found a therapeutic use. The safety of benzodiazepines may indicate an important advantage of allosterically acting agents, compared with those acting competitively; their effect has a limit, i.e., the allosteric constant for the agent, receptor, and endogenous agonist. This limit allows, in principle, agents with absolute selectivity. A competitive muscarinic antagonist may be subtype selective but must inhibit all subtypes completely at a sufficiently high concentration; an allosteric agent that is inhibitory at one subtype but neutrally cooperative at the rest would affect only the single subtype up to a certain maximal extent, even at supramaximally effective concentrations. Similarly, an allosteric agent could enhance the affinity of the endogenous agonist to a limited extent at one subtype while having no functional effect at the other subtypes. Such an agent, effective at m1 receptors, could have therapeutic value in Alzheimer's disease.

The allosteric effect of an agent at a particular receptor depends upon the particular ligand occupying the primary binding site (2, 9, 23). A therapeutic allosteric agent would interact with the endogenous agonist but, in most cases, allosteric action has been measured with synthetic radioligands and little, if anything, is known about allosteric effects with the endogenous unlabeled agonist [although PD81,723 [2-amino-4,5-dimethylthien-3-yl(3-trifluoromethylphenyl)-methanone] has been shown to enhance the affinity of adenosine at A_1 receptors] (24). Here, we have described procedures for the detection and quantitation of allosteric actions with an unlabeled endogenous agonist at a G protein-coupled receptor, using the interaction between strychnine and ACh at muscarinic receptors as an example.

Strychnine, like alcuronium, increases the affinity of [^{3}H]NMS at m2 receptors (9) but, unlike alcuronium, it is neutrally or only slightly negatively cooperative at m1 and m3 receptors, i.e., it binds to the receptors without greatly altering the affinity of [^{3}H]NMS, although it does profoundly alter the kinetics of [^{3}H]NMS binding. In contrast, it has a small degree of negative cooperativity with ACh (2–7-fold), with the largest effects at m2 and m3 receptors. It has an affinity of about 10^5 M^{-1} at m1, m2, and m4 receptors and is weaker at m3 receptors. Functionally, strychnine reduced ACh potency for stimulating [^{35}S]GTPγS binding but it also reduced basal activity and E_{max}, which prevented more detailed analysis.

The properties of strychnine were initially measured in an assay in which the amount of [^{3}H]NMS bound in the presence of an agent, or in the presence of agent and unlabeled ACh, was transformed into an estimate of the affinity ratio of the signal ([^{3}H]NMS or ACh). This measure is, in principle, independent of the concentration of signaling ligands. The graphical output from this assay therefore allows a direct visual comparison of the effects of an agent on both [^{3}H]NMS and ACh binding; if the effects differ then the agent may be acting allosterically. In addition, the fractional effect of the

agent on the affinity ratio corresponds to the fractional occupancy of the receptor by the agent in the absence of other ligands, so if the agent is strongly negatively cooperative (with either ligand) or competitive its IC_{50} can be read from the plot and corresponds to its dissociation constant.

The affinity of strychnine and its allosteric effects on [^{3}H]NMS and ACh affinity were quantified more accurately by measuring ACh inhibition curves for [^{3}H]NMS binding alone and in the presence of various concentrations of strychnine. The raw data were fitted directly to the ternary complex model of allosteric action. The good fits we obtained provide support for an allosteric mode of action, because the fit must account for the effects on both [^{3}H]NMS and ACh binding.

Like other allosteric agents at muscarinic receptors, strychnine slows the rate of dissociation of [^{3}H]NMS to a value close to 0. We have shown that, if the agent has sufficiently rapid kinetics, the fractional inhibition of [^{3}H]NMS k_{off} by a particular concentration of agent corresponds to the fractional occupancy by the agent of the [^{3}H]NMS-occupied receptor. If the agent strongly inhibits this measure, its IC_{50} corresponds to its dissociation constant at the [^{3}H]NMS-occupied receptor. The cooperativity of the agent with [^{3}H]NMS is the ratio of its affinities for [^{3}H]NMS-occupied and free receptors (7) and, in the case of strychnine, the estimates of affinity for the [^{3}H]NMS-occupied receptor from the equilibrium experiments agree well with those measured experimentally, again supporting the allosteric model.

Results obtained with strychnine and alcuronium in a different nonequilibrium assay were also consistent with the allosteric model. This assay uses prelabeled and initially unlabeled receptors to detect both kinetic and equilibrium effects of the agent; it allows the estimation of the affinity and allosteric interactions of agents that are positively cooperative with [^{3}H]NMS and that slow [^{3}H]NMS association sufficiently to preclude the attainment of binding equilibrium.

We derived an equation that allows functional concentration-effect curve data obtained with ACh in the absence and presence of various concentrations of allosteric agent to be analyzed directly with nonlinear regression. The equation is an extended form of the integrated Schild/logistic equation used to analyze data obtained with competitive antagonists (25–27). The assumptions underlying the use of these equations are the same as for Schild analysis, together with the requirement that the agonist curve can be described by a logistic function. Analysis of the data by fitting the entire data set directly to the equation is more efficient, and less distorting, than fitting each curve individually to a logistic function and then fitting the EC_{50} values to the allosteric model (7). Using ACh stimulation of [^{35}S]GTPγS binding as the functional response, we obtained values for the affinity of gallamine at m2 receptors and its allosteric effect with ACh that are in good agreement with published values. It was not possible to obtain comparable parameter estimates for strychnine, however, because at high concentrations it reduced basal and maximal response levels.

By studying the effects of an agent on two ligands, radioligand and unlabeled agonist, and using different assay systems to measure the cooperativity parameters, we can determine whether the behavior of the agent is fully consistent with the allosteric model. The data for strychnine are internally consistent and support the claim that strychnine acts allosterically at muscarinic receptors. There may be at least three regions of the muscarinic receptor that bind allosteric agents (14, 28), and methods have been described for assessing whether allosteric agents act at a common site (29, 30). The location and pharmacological characteristics of the strychnine binding sites on muscarinic receptors have yet to be determined.

Agents acting allosterically with the endogenous transmitter for G protein-coupled receptors may have therapeutic value, but the detection and quantitation of such agents are more taxing than the detection of simple agonists or antagonists. The procedures and theory described in this paper may help the search.

Appendix

A. Ternary complex model of allosteric action with two competitive ligands and one allosteric agent. The model consists of a receptor with two binding sites, i.e., one for muscarinic ligands and the second for allosteric ligands. The two types of ligand can bind simultaneously, and the affinity of one type of ligand for the receptor may be different from its affinity when the receptor is occupied by the other type of ligand. This is the allosteric effect of one ligand on the other.

$$\begin{array}{ccccc} X & & X & & X \\ + & & + & & + \\ LR & \overset{K_L}{\Leftrightarrow} & L + R + A & \overset{K_A}{\Leftrightarrow} & AR \\ {\scriptstyle \alpha K_X}\Updownarrow & & \Updownarrow{\scriptstyle K_X} & & \Updownarrow{\scriptstyle \beta K_X} \\ LRX & \underset{\alpha K_L}{\Leftrightarrow} & L + RX + A & \underset{\beta K_A}{\Leftrightarrow} & ARX \end{array}$$

In the above scheme, radioligand L binds to receptor R in the presence of competitive ligand A and a second agent X, which binds to a different site on the receptor. K_L, K_A, and K_X are affinity constants; α and β are the allosteric constants of L and A, respectively, with X.

There is a fundamental constraint on the allosteric effect of one type of ligand on the other; it must be the same for both ligands. Therefore, the maximal allosteric effect, α, of X on L is the ratio of the affinities of L for the X-occupied receptor and the free receptor, and it is also the ratio of the affinities of X for the L-occupied receptor and the free receptor. It is assumed that ligands are present in excess, i.e., the free ligand concentrations are always the same as the total ligand concentration.

B. Binding of radioligand under equilibrium conditions in the presence of unlabeled competitor and allosteric agent. R_t is the total receptor population, R is the concentration of free receptor, LR, AR, etc., are the concentrations of the various bound receptor species, A, L, and X are the free concentrations of competitor, radioligand, and allosteric agent, respectively, B_L, B_{LX}, B_{LA}, and B_{LAX} are concentrations of radioligand bound to receptor alone, in the presence of X, in the presence of A, and in the presence of both A and X, respectively, α is the allosteric constant for X and L, and β is the allosteric constant for X and A.

$$R_t = R + LR + AR + RX + LRX + ARX$$

where

$$LR = R \cdot L \cdot K_L$$

$$AR = R \cdot A \cdot K_A$$

$$RX = R \cdot X \cdot K_X$$

$$LRX = R \cdot \alpha \cdot L \cdot X \cdot K_L \cdot K_X$$

$$ARX = R \cdot \beta \cdot A \cdot X \cdot K_A \cdot K_X$$

In the presence of both ligands, bound radioligand is

$$LR + LRX = B_{LAX}$$

and, therefore,

$$\frac{B_{LAX}}{R_t} = \frac{LR + LRX}{R + LR + AR + RX + LRX + ARX}$$

and the general equation for the binding of radioligand in the presence of competitor and allosteric agent is given by

$$B_{LAX} = R_t \cdot \frac{L \cdot K_L \cdot (1 + \alpha \cdot X \cdot K_X)}{1 + X \cdot K_X + A \cdot K_A \cdot (1 + \beta \cdot X \cdot K_X) + L \cdot K_L \cdot (1 + \alpha \cdot X \cdot K_X)} \quad (1)$$

By omitting terms containing competitor (A) and/or allosteric agent (X), we obtain the binding of radioligand in the presence of allosteric agent,

$$B_{LX} = R_t \cdot \frac{L \cdot K_L \cdot (1 + \alpha \cdot X \cdot K_X)}{1 + X \cdot K_X + L \cdot K_L \cdot (1 + \alpha \cdot X \cdot K_X)} \quad (2)$$

the binding of radioligand in the presence of competitor,

$$B_{LA} = R_t \cdot \frac{L \cdot K_L}{1 + A \cdot K_A + L \cdot K_L} \quad (3)$$

and the binding of radioligand alone

$$B_L = R_t \cdot \frac{L \cdot K_L}{1 + L \cdot K_L} \quad (4)$$

C. Calculation of the apparent affinity of radioligand and competitor in the presence of an allosteric agent and the 'affinity ratio' measure. This section describes the calculations used in the semiquantitive equilibrium assay (see Experimental Procedures) to derive the affinity ratio (apparent ligand affinity/true ligand affinity) of radioligand and unlabeled ligand in the presence of allosteric agent. Radioligand binding is measured alone and in the presence of a range of concentrations of allosteric agent, alone (B_{LX}) and in the presence (B_{LAX}) of a fixed concentration of unlabeled competitive ligand; binding of a high concentration of radioligand is also measured, together with nonspecific binding with both high and low radioligand concentrations. The following derivation applies to specific binding (total binding observed minus nonspecific binding measured with the same concentration of radioligand).

The binding curves described in eqs. 1–4 all have the form

$$B = R_t \cdot \frac{L \cdot K}{1 + L \cdot K}$$

a simple binding function, where K is the apparent affinity of L under the specified conditions (1/concentration giving 50% of maximal binding).

From eq. 2, the apparent affinity of radioligand in the presence of allosteric agent is

$$K_{LX} = \frac{K_L \cdot (1 + \alpha \cdot X \cdot K_X)}{1 + X \cdot K_X} \quad (5)$$

Substituting the binding constants of the competitor into eq. 5, the apparent affinity of competitor in the presence of allosteric agent is

$$K_{AX} + \frac{K_A \cdot (1 + \beta \cdot X \cdot K_X)}{1 + X \cdot K_X} \quad (6)$$

K_{LX} and K_{AX} are the parameters to be calculated.

First the receptor concentration, R_t, is calculated, using the values of specific radioligand binding, B_{L_1} and B_{L_2}, at two free concentrations of radioligand, L_1 and L_2, in the absence of A and X.

From eq. 4,

$$B_{L_1} = \frac{R_t \cdot L_1 \cdot K_L}{1 + L_1 \cdot K_L} \quad \text{and} \quad B_{L_2} = \frac{R_t \cdot L_2 \cdot K_L}{1 + L_2 \cdot K_L}$$

R_t is obtained by solving for K_L, equating, and rearranging.

$$R_t = \frac{B_{L_1} \cdot B_{L_2} \cdot (L_2 - L_1)}{L_2 \cdot B_{L_1} - L_1 \cdot B_{L_2}} \quad (7)$$

The value of R_t is used to transform B_{LX}, specific binding in the presence of X, into K_{LX}.

$$B_{LX} = R_t \cdot \frac{L \cdot K_{LX}}{1 + L \cdot K_{LX}} \quad (8)$$

Rearranging eq. 8, K_{LX}, the apparent affinity of L in the presence of X, is calculated using the values of L, R_t, and B_{LX},

$$K_{LX} = \frac{B_{LX}}{L \cdot (R_t - B_{LX})} \quad (9)$$

The specific binding measured in the presence of A and X, B_{LAX}, is then transformed into K_{AX}, using the values of R_t and B_{LX}.

Substituting eqs. 5 and 6 into eq. 1, we obtain

$$B_{LAX} = R_t \cdot \frac{L \cdot K_{LX}}{1 + A \cdot K_{AX} + L \cdot K_{LX}} \quad (10)$$

By rearrangement of eq. 10, we obtain

$$K_{AX} = \frac{1}{A} \cdot \left[\frac{R_t \cdot L \cdot K_{LX}}{B_{LAX}} - (1 + L \cdot K_{LX}) \right] \quad (11)$$

By rearrangement of eq. 9, we obtain

$$1 + L \cdot K_{LX} = \frac{R_t}{R_t - B_{LX}} \quad \text{and} \quad L \cdot K_{LX} = \frac{B_{LX}}{R_t - B_{LX}} \quad (12)$$

By substituting eq. 12 into eq. 11 and rearranging, K_{AX}, the apparent affinity of A in the presence of X, is calculated using the values of A, R_t, B_{LX}, and B_{LAX}

$$K_{AX} = \frac{R_t \cdot (B_{LX} - B_{LAX})}{A \cdot B_{LAX} \cdot (R_t - B_{LX})} \quad (13)$$

The affinity ratio of L or A, r_L or r_A, respectively, is the apparent affinity of the ligand in the presence of X expressed as a fraction of the true affinity (measured in the absence of X), i.e., K_{LX}/K_L or K_{AX}/K_A, respectively.

D. Relationship between the concentration of allosteric agent and the affinity ratio. We consider the affinity ratio of L in the presence of X, r_L. The same arguments apply to r_A.

$$r_L = \frac{K_{LX}}{K_L} \quad (14)$$

Substituting eq. 5 into eq. 14, we obtain

$$r_L = \frac{1 + \alpha \cdot X \cdot K_X}{1 + X \cdot K_X} \quad (15)$$

For $X = 0$, the affinity ratio is

$$r_{L\,\mathrm{min}} = 1 \quad (16)$$

For $X \gg K_X$, the affinity ratio is

$$r_{L\,\mathrm{max}} = \alpha \quad (17)$$

The fractional effect of X, relative to its own maximum, eff_X, is given by

$$\mathrm{eff}_X = \frac{1 - r_L}{1 - \alpha} \quad \text{or equally} \quad \mathrm{eff}_X = \frac{r_L - 1}{\alpha - 1} \quad (18)$$

By substitution of eq. 15 into eq. 18 and rearangement, the fractional effect of X on the affinity ratio of L is

$$\mathrm{eff}_x = \frac{X \cdot K_X}{1 + X \cdot K_X} \quad (19)$$

The fractional effect of X on r_L therefore corresponds to occupancy by X of the free receptor in the absence of any other ligand.

Note that with $\alpha \ll 1$, i.e., X is strongly negatively allosteric or competitive, $\mathrm{eff}_X = 1 - r_L$, and the IC_{50} of the plot of affinity ratio versus concentration of X corresponds to 1/affinity of X for the free receptor. Note also that eq. 19 is independent of the ligand concentration or cooperativity with X and applies equally to r_A, the affinity ratio of the unlabeled competitor in the presence of X. Curves of r_L and r_A versus X should have the same EC_{50} ($1/K_X$) and should overlap unless $\alpha \neq \beta$.

E1. Radioligand dissociation in the presence of an allosteric agent that slows dissociation. B_{LX} is bound L in the presence of X (XRL + RL) at equilibrium (eq. 2), B_{LX_t} is bound L in the presence of X at time t after dissociation has started, k_{off} is the rate constant for dissociation of L from unoccupied receptors (RL), k_{off_X} is the rate constant for dissociation of L from receptors with bound X (XRL), $k_{off_{obs}}$ is the observed dissociation rate constant of L, αK_X is the affinity of X for RL, i.e., for the [^{3}H]NMS-occupied receptor, and q is the fractional occupancy of B_{LX} by X,

$$q = \frac{X \cdot \alpha \cdot K_X}{1 + X \cdot \alpha \cdot K_X} \quad (20)$$

The fraction of B_{LX} not occupied by X equals $(1 - q)$.

The effect of the allosteric agent on the pattern of radioligand dissociation depends on the kinetics of the agent. In addition, if X has fast binding kinetics it equilibrates rapidly with prelabeled receptors, whereas if X has slow binding kinetics it must be present during receptor labeling to ensure that equilibrium is reached. We have explored the problem with numerical simulation, and here we consider the two limiting cases, the first resulting in a biphasic curve and the second in a monophasic curve.

If X has slow binding kinetics and there is negligible dissociation of X from XRL during the period in which dissociation of L is observed, then RL and XRL behave as distinct populations and fractional occupancy of B_{LX} by X, q, increases as RL dissociates.

$$B_{LX_t} = B_{LX} \cdot [q \cdot \exp(-t \cdot k_{off_X}) + (1 - q) \cdot \exp(-t \cdot k_{off})]$$

If the rate constant for the dissociation of X from XRL is within about 1 order of magnitude of k_{off}, then biphasic dissociation curves are also seen, but these are difficult to interpret without knowlege of the kinetic constants of the allosteric agent.

If X has fast binding kinetics, then fractional occupancy of B_{LX} by X, q, remains constant as RL dissociates

$$\frac{d}{dt} B_{LX_t} = B_{LX_t} \cdot [q \cdot k_{off_X} + (1 - q) \cdot k_{off}]$$

By integration, the bound radioligand at time t, B_{LX_t}, is given by

$$B_{LX_t} = B_{LX} \cdot \exp[-t \cdot [q \cdot k_{off_X} + (1 - q) \cdot k_{off}]]$$

and the observed dissociation rate constant, $k_{off_{obs}}$, is

$$k_{off_{obs}} = q \cdot k_{off_X} + (1 - q) \cdot k_{off} \quad (21)$$

By substitution of eq. 20 into eq. 21, the observed radioligand dissociation rate constant in the presence of an allosteric agent, $k_{off_{obs}}$, is

$$k_{off_{obs}} = \frac{X \cdot \alpha \cdot K_X \cdot k_{off_X} + k_{off}}{1 + X \cdot \alpha \cdot K_X} \quad (22)$$

The complete equation describing the amount of bound radioligand, B_{LX_t}, after a period of dissociation, t, in the presence of a concentration of allosteric agent, X, with initial binding of B_{LX}, is

$$B_{LX_t} = B_{LX} \cdot \exp\left(-t \cdot \frac{X \cdot \alpha \cdot K_X \cdot k_{off_X} + k_{off}}{1 + X \cdot \alpha \cdot K_X}\right) \quad (23)$$

E2. Relationship between inhibition of k_{off} and occupancy by X of the liganded receptor. From eq. 22, when $X = 0$, $k_{off_{obs}} = k_{off}$ and when $X \gg 1/\alpha K_X$, $k_{off_{obs}} = k_{off_X}$. Fractional inhibition of k_{off} is

$$\frac{k_{off} - k_{off_{obs}}}{k_{off} - k_{off_X}} = \frac{X \cdot \alpha \cdot K_X}{1 + X \cdot \alpha \cdot K_X}$$

which is eq. 20, the fractional occupancy by X of B_{LX}. The fractional inhibition of radioligand dissociation rate constant by an allosteric agent, relative to its own maximal effect, therefore corresponds to the occupancy by the agent of the liganded receptor, as long as the agent dissociates from the receptor >10 times faster than the radioligand.

For $k_{off_X} \ll k_{off}$, a high concentration of X almost completely inhibits the dissociation of L. By simplifying eq. 22, the observed radioligand dissociation rate constant in the presence of an allosteric agent, with $k_{off_X} \ll k_{off}$, is given by

$$k_{off_{obs}} = \frac{k_{off}}{1 + X \cdot \alpha \cdot K_X} \quad (24)$$

and the concentration of agent that slows k_{off} by 50% corresponds to $1/(\alpha K_X)$. Note that if the agent increases radioligand k_{off} then eqs. 22 and 23, and the relationship between fractional effect and fractional occupancy, remain valid.

F1. Effect of an allosteric agent on the association rate of [^{3}H]NMS. The inhibition by X of the [^{3}H]NMS dissociation rate also affects its association rate and, at high concentrations of allosteric agent, radioligand binding is not in equilibrium. It is useful to be able to recognize this and to predict such kinetic artifacts.

Again, we assume that the kinetics of the allosteric agent are much more rapid than those of the radioligand and that the binding of [^{3}H]NMS can be described by a simple bimolecular process, i.e., not involving slow isomerization. k_{on} is the molecular association rate constant for [^{3}H]NMS, and k_{obs} is the experimentally observed rate constant for [^{3}H]NMS association. In the absence of allosteric agent

$$k_{obs} = k_{off} + L \cdot k_{on}$$

Because affinity, K_L, equals k_{on}/k_{off}, the observed association rate constant can be expressed as

$$k_{obs} = k_{off} \cdot (1 + L \cdot K_L) \quad (25)$$

Note that this relationship is itself quite useful; it allows the half-time for association $[-\ln(0.5)/k_{obs}]$ to be predicted from a knowledge of K_L and k_{off}, and it shows that the rate of binding of low concentrations of L approaches the dissociation rate constant.

In the presence of X, by substitution into eq. 25, the observed association rate constant is

$$k_{obs_X} = k_{off_{obs}} \cdot (1 + L \cdot K_{LX}) \quad (26)$$

K_{LX} is defined in eq. 5 and $k_{off_{obs}}$ is defined in eq. 22 or eq. 24.

Binding of L in the presence of X at time t after the initiation of association, B_{LX_t}, is therefore given by

$$B_{LX_t} = B_{LX} \cdot [1 - \exp(-t \cdot k_{obs_X})] \quad (27)$$

B_{LX} is defined in eq. 2.

F2. Effect of an allosteric agent and a competitor on the association rate of [^{3}H]NMS. The effect of an unlabeled competitor, A, on the rate of radioligand association depends on the dissociation rate of the competitor (15). If this is slower than or about the same as the dissociation rate of the radioligand, then radioligand binding is a complex function of time. If the competitor has much faster kinetics than the radioligand, however, then radioligand association is a monoexponential function of time. The k_{obs} of radioligand can then be calculated from the apparent radioligand affinity in the presence of X and A, as in eq. 26.

The apparent affinity of L in the presence of A and X, from eq. 1, is

$$K_{LAX} = \frac{K_L \cdot (1 + \alpha \cdot X \cdot K_X)}{1 + X \cdot K_X + A \cdot K_A \cdot (1 + \beta \cdot X \cdot K_X)} \quad (28)$$

The observed association rate constant in the presence of A and X is

$$k_{obs_{AX}} = k_{off_{obs}} \cdot (1 + L \cdot K_{LAX}) \quad (29)$$

where $k_{off_{obs}}$ is defined in eq. 22 or eq. 24, and the binding of L in the presence of A and X at time t, B_{LAX_t}, is given by

$$B_{LAX_t} = B_{LAX} \cdot [1 - \exp(-t \cdot k_{obs_{AX}})] \quad (30)$$

where B_{LAX} is defined in eq. 1.

F3. Time needed for radioligand binding equilibrium in the presence of an agent that slows kinetics. It is useful to estimate the time needed for an acceptable approach to equilibrium binding (e.g., 5 half-lives). If the concentration of L is $\ll 1/K_L$ or a high concentration of unlabeled competitor with faster kinetics is also present, then the association rate of L approaches its dissociation rate (15), so, to ensure that all binding is in equilibrium, we can assume that the minimum k_{obs} is k_{off}. We also assume that k_{off_X} is negligible (see eq. 24).

If $t_{0.5_{off}}$ is the half-time for radioligand dissociation from the free receptor, then a conservative estimate of radioligand association half-time in the presence of allosteric agent is given by

$$t_{0.5_{obs_X}} = t_{0.5_{off}} \cdot (1 + \alpha \cdot X \cdot K_X) \quad (31)$$

G. Estimation of affinity and allosteric constants of allosteric agents that slow radioligand kinetics and are positively or neutrally cooperative with the radioligand, using prelabeling with radioligand. An allosteric agent that slows radioligand kinetics does so at concentrations approaching and above the dissociation constant (1/affinity) of the agent for the liganded receptor. If the affinity of the agent at the liganded receptor is higher than or similar to its affinity at the free receptor (i.e., it has positive or approximately neutral cooperativity with the radioligand), then the concentrations of agent that are needed to accurately measure its affinity and cooperativity with radioligand (and negative cooperativity with unlabeled competitor) slow the association kinetics of the radioligand so much that binding equilibrium is unattainable. If this occurs in studies assumed to measure equilibrium binding, then the inhibition of binding that occurs is a kinetic artifact, although it may be misinterpreted as allosteric (or competitive) inhibition. Analysis of data containing kinetic artifacts with an equilibrium model results in erroneous parameter estimates.

The possibility of a kinetic artifact can be assessed by labeling the receptors with radioligand before exposure to the agent and comparing the binding obtained after an additional incubation period with binding obtained with the same incubation period under normal 'equilibrium' conditions. In addition to detecting kinetic effects, this design makes use of these effects to quantitate the affinity and allosteric constant(s) of the agent.

Experimentally, membranes and radioligand are prepared at 100 times the final concentrations, and tubes are prepared containing 1 ml of allosteric agent at its final concentration. Half of the membranes and radioligand are mixed. There are two sets of tubes. The tubes of set A receive 20 μl of the mixture. The tubes of set B receive 10 μl of radioligand followed by 10 μl of membranes. The high initial radioligand concentration under the first conditions (50-fold higher than during the main incubation) causes rapid labeling of almost the entire receptor population.

Radioligand binding in the presence of an allosteric agent approaches equilibrium exponentially, with a rate constant of k_{obs_X} (eq. 26), regardless of whether preequilibrium binding is less than or greater than equilibrium binding. The theoretical equilibrium binding, B_{LX}, is defined in eq. 2.

For set A, preequilibriated binding is

$$B_{L_{hi}} = \frac{R_t \cdot L \cdot 50 \cdot K_L}{1 + L \cdot 50 \cdot K_L} \tag{32}$$

Bound radioligand at time t in set A is

$$B_{LX_t} = B_{LX} + (B_{L_{hi}} - B_{LX}) \cdot \exp(-t \cdot k_{obs_X})$$

$$B_{LX_t} = B_{LX} \cdot [1 - \exp(-t \cdot k_{obs_X})] + B_{L_{hi}} \cdot \exp(-t \cdot k_{obs_X}) \tag{33}$$

For set B, B_{LX_t} is defined in eq. 27, which is the same as eq. 33 when $B_{L_{hi}} = 0$.

Simultaneous nonlinear regression analysis of data sets A and B using eqs. 33 and 27, respectively, with radioligand concentration and incubation time as fixed constants, gives estimates of the following parameters: R_t, K_L, k_{off}, k_{off_X}, K_X, and α. The estimate of k_{off_X} may not differ significantly from 0 or may not be well defined, in which case k_{off_X} can be fixed at 0.

If the agent has neutral cooperativity with the radioligand, then estimates of the affinity of the agent (K_X) are highly correlated with estimates of radioligand k_{off}, and the latter estimates may well be inaccurate. In that case k_{off} should be fixed at its known value. Similarly, it may be necessary to fix the value of K_L to the known radioligand affinity if the value of R_t is not well defined by the data.

The experimental design can be extended to allow the estimation of allosteric interaction with an unlabeled competitor. Tubes of a third group, set C, containing 1 ml of allosteric agent plus a fixed concentration of competitor, receive 10 μl of radioligand followed by 10 μl of receptors. If the competitor is an agonist then GTP is included throughout. The appropriate choice of competitor concentration depends on the magnitude and direction (positive or negative) of the cooperativity with the agent. For set C, B_{LAX_t} is defined in eq. 30. Simultaneous analysis of data sets A, B, and C using eqs. 33, 27, and 30, respectively, gives the following additional parameter estimates: K_A and β.

The inhibitor may, like ACh in the current studies, inhibit radioligand binding with a Hill slope different from unity (see below). In this case the slope factor may be built into the model if required, but this affects only the estimate of K_A; it does not affect the estimate of β or the other parameters.

H. Effects of an allosteric agent on ACh in binding and functional studies. In *binding* studies in the presence of GTP, unlabeled ACh often inhibits antagonist radioligand binding with a Hill slope of <1 (0.8–1). Whatever the explanation for this phenomenon, we assume that the curve is a function of ACh affinity. We therefore modify eq. 1 by treating ACh binding as a logistic function with a slope factor of n.

Bound radioligand =

$$R_t \cdot \frac{L \cdot K_L \cdot (1 + \alpha \cdot X \cdot K_X)}{1 + X \cdot K_X + (A \cdot K_A)^n \cdot (1 + \beta \cdot X \cdot K_X) + L \cdot K_L \cdot (1 + \alpha \cdot X \cdot K_X)} \tag{34}$$

Fitting the data from the quantitative equilibrium assay (see Experimental Procedures) to eq. 34 yields estimates for K_L, K_A, n, K_X, α, and β, given R_t and L as constants with A and X as independent variables.

In *functional* studies we assume that the allosteric agent affects only ACh affinity, with no effect on efficacy, that the agent does not affect basal activity, maximal agonist effect, or the shape of the agonist curve, that ACh (A) and the allosteric agent (X) bind according to the law of mass action, and that the ACh concentration-effect curve can be described by a logistic function.

Basal is the effect measured in the absence of A, E_{max} is the effect measured with a maximally effective concentration of A, EC_{50} is the concentration of ACh, in the absence of allosteric agent, causing a 50% maximal response, and n is the slope factor of the logistic function describing the effect of A. Equieffective concentrations of ACh in the presence of allosteric agent are referred to as A′ or EC_{50}'.

In the absence of allosteric agent, fractional receptor occupancy by A (from eq. 4) is

$$\text{Fractional occupancy} = \frac{A \cdot K_A}{1 + A \cdot K_A}$$

In the presence of allosteric agent, fractional receptor occupancy by A is

$$\text{Fractional occupancy} = \frac{A \cdot K_{AX}}{1 + A \cdot K_{AX}}$$

where

$$K_{AX} = \frac{K_A \cdot (1 + \beta \cdot X \cdot K_X)}{1 + X \cdot K_X}$$

(see eq. 6).

If agonist concentrations A and A′, in the absence and presence of agent, respectively, have the same effect, i.e., result in the same receptor occupancy, then

$$A' \cdot K_{AX} = A \cdot K_A$$

and the dose ratio in the presence of agent is

$$\frac{A'}{A} = \frac{1 + X \cdot K_X}{1 + \beta \cdot X \cdot K_X} \tag{35}$$

When the effect is measured at the 50% level, then the EC_{50} in the presence of agent is

$$EC_{50}' = EC_{50} \cdot \frac{1 + X \cdot K_X}{1 + \beta \cdot X \cdot K_X} \tag{36}$$

If the effect of the agonist can be described by a logistic

function then, in general,

$$\text{Effect} = \text{basal} + \frac{E_{max} - \text{basal}}{1 + \left(\frac{EC_{50}'}{A}\right)^n}$$

By substitution into eq. 36, we obtain the functional effect of ACh in the presence of allosteric agent,

$$\text{Effect} = \text{basal} + \frac{E_{max} - \text{basal}}{1 + \left(\frac{EC_{50}}{A} \cdot \frac{1 + X \cdot K_X}{1 + \beta \cdot X \cdot K_X}\right)^n} \quad (37)$$

Fitting the functional data set to eq. 37 yields estimates of basal, E_{max}, β, K_X, and n, given A and X as independent variables. If the agent is competitive, then $\beta = 0$ and eq. 37 becomes the integrated Schild/logistic equation (25–27).

Note Added in Proof

The Appendix of this paper is available as a Mathcad document on the World Wide Web, at http://www.nimr.mrc.ac.uk/CC/molpharm/alloster.html.

References

1. Hulme, E. C., N. J. M. Birdsall, and N. J. Buckley. Muscarinic receptor subtypes. *Annu. Rev. Pharmacol. Toxicol.* **30:**633–673 (1990).
2. Stockton, J. M., N. J. M. Birdsall, A. S. Burgen, and E. C. Hulme. Modification of the binding properties of muscarinic receptors by gallamine. *Mol. Pharmacol.* **23:**551–557 (1983).
3. Ellis, J., J. Huyler, and M. R. Brann. Allosteric regulation of cloned m1–m5 muscarinic receptor subtypes. *Biochem. Pharmacol.* **42:**1927–1932 (1991).
4. Lee, N. H., and E. E. el-Fakahany. Allosteric antagonists of the muscarinic acetylcholine receptor. *Biochem. Pharmacol.* **42:**199–205 (1991).
5. Ariens, E. J., J. M. Van Rossum, and A. M. Simonis. A theoretical basis of molecular pharmacology. *Arzneim. Forsch.* **6:**611–621 (1956).
6. van den Brink, F. G. General theory of drug-receptor interactions. *Handb. Exp. Pharmacol.* **47:**169–254 (1977).
7. Ehlert, F. J. Estimation of the affinities of allosteric ligands using radioligand binding and pharmacological null methods. *Mol. Pharmacol.* **33:** 187–194 (1988).
8. Ehlert, F. J. Gallamine allosterically antagonizes muscarinic receptor-mediated inhibition of adenylate cyclase activity in the rat myocardium. *J. Pharmacol. Exp. Ther.* **247:**596–602 (1988).
9. Tuček, S., J. Musílková, J. Nedoma, J. Proška, S. Shelkovnikov, and J. Vorlíček. Positive cooperativity in the binding of alcuronium and *N*-methylscopolamine to muscarinic acetylcholine receptors. *Mol. Pharmacol.* **38:**674–680 (1990).
10. Proška, J., and S. Tuček. Mechanisms of steric and cooperative actions of alcuronium on cardiac muscarinic acetylcholine receptors. *Mol. Pharmacol.* **45:**709–717 (1994).
11. Bruns, R. F. Receptor binding studies in drug discovery: problems, solutions and opportunities, in *Biology of Actinomycetes '88* (Y. Okami, T. Beppu, and H. Ogawara, eds.). Japan Scientific Societies Press, Tokyo, 165–170 (1988).
12. Birdsall, N. J. M., F. Cohen, S. Lazareno, and H. Matsui. Allosteric regulation of G-protein linked receptors. *Biochem. Soc. Trans.* **23:**108–111 (1995).
13. Buckley, N. J., T. I. Bonner, C. M. Buckley, and M. R. Brann. Antagonist binding properties of five cloned muscarinic receptors expressed in CHO-K1 cells. *Mol. Pharmacol.* **35:**469–476 (1989).
14. Leppik, R. A., R. C. Miller, M. Eck, and J. L. Paquet. Role of acidic amino acids in the allosteric modulation by gallamine of antagonist binding at the m2 muscarinic acetylcholine receptor. *Mol. Pharmacol.* **45:**983–990 (1994).
15. Motulsky, H. J., and L. C. Mahan. The kinetics of competitive radioligand binding predicted by the law of mass action. *Mol. Pharmacol.* **25:**1–9 (1984).
16. Matsui, H., S. Lazareno, and N. J. M. Birdsall. Probing of the location of the allosteric site on m1 muscarinic receptors by site-directed mutagenesis. *Mol. Pharmacol.* **47:**88–98 (1995).
17. Hilf, G., P. Gierschik, and K. H. Jakobs. Muscarinic acetylcholine receptor-stimulated binding of guanosine 5′-*O*-(3-thiotriphosphate) to guanine-nucleotide-binding proteins in cardiac membranes. *Eur. J. Biochem.* **186:** 725–731 (1989).
18. Lazareno, S., T. Farries, and N. J. M. Birdsall. Pharmacological characterization of guanine nucleotide exchange reactions in membranes from CHO cells stably transfected with human muscarinic receptors m1–m4. *Life Sci.* **52:**449–456 (1993).
19. Clark, A. L., and F. Mitchelson. The inhibitory effect of gallamine on muscarinic receptors. *Br. J. Pharmacol.* **58:**323–331 (1976).
20. Nunnari, J. M., M. G. Repaske, S. Brandon, E. J. Cragoe, Jr., and L. E. Limbird. Regulation of porcine brain α_2-adrenergic receptors by Na^+, H^+ and inhibitors of Na^+/H^+ exchange. *J. Biol. Chem.* **262:**12387–12392 (1987).
21. Bruns, R. F., and J. H. Fergus. Allosteric enhancement of adenosine A_1 receptor binding and function by 2-amino-3-benzoylthiophenes. *Mol. Pharmacol.* **38:**939–949 (1990).
22. Neve, K. A. Regulation of dopamine D_2 receptors by sodium and pH. *Mol. Pharmacol.* **39:**570–578 (1991).
23. Christopoulos, A., and F. Mitchelson. Assessment of the allosteric interactions of the bisquaternary heptane-1,7-bis(dimethyl-3′-phthalimidopropyl)ammonium bromide at M1 and M2 muscarine receptors. *Mol. Pharmacol.* **46:**105–114 (1994).
24. Cohen, F., S. Lazareno, and N. J. M. Birdsall. Allosteric interactions of PD81,723 at the human adenosine A_1 receptor. *Br. J. Pharmacol.* **113:** 51P.
25. Waud, D. R. Analysis of dose-response curves. *Methods Pharmacol.* 471–506 (1975).
26. Lazareno, S., and N. J. M. Birdsall. Estimation of competitive antagonist affinity from functional inhibition curves using the Gaddum, Schild and Cheng-Prusoff equations. *Br. J. Pharmacol.* **109:**1110–1119 (1993).
27. Lazareno, S., and N. J. M. Birdsall. Estimation of antagonist K_b from inhibition curves in functional experiments: alternatives to the Cheng-Prusoff equation. *Trends Pharmacol. Sci.* **14:**237–239 (1993).
28. Potter, L. T., C. A. Ferrendelli, H. E. Hanchett, M. A. Hollifield, and M. V. Lorenzi. Tetrahydroaminoacridine and other allosteric antagonists of hippocampal M1 muscarine receptors. *Mol. Pharmacol.* **35:**652–660 (1989).
29. Ellis, J., and M. Seidenberg. Two allosteric modulators interact at a common site on cardiac muscarinic receptors. *Mol. Pharmacol.* **42:**638–641 (1992).
30. Waelbroeck, M. Identification of drugs competing with *d*-tubocurarine for an allosteric site on cardiac muscarinic receptors. *Mol. Pharmacol.* **46:** 685–692 (1994).
31. Munson, P. J., and D. Rodbard. LIGAND: a versatile computerized approach for characterization of ligand-binding systems. *Anal. Biochem.* **107:**220–239 (1980).

Send reprint requests to: Sebastian Lazareno, MRC Collaborative Centre, Mill Hill, London NW7 1AD, UK.